C.P. No. 845

C.P. No. 845

MINISTRY OF AVIATION

AERONAUTICAL RESEARCH COUNCIL

CURRENT PAPERS

The Lateral Oscillation of Slender Aircraft

by

A. J. Ross, Ph.D.

LONDON: HER MAJESTY'S STATIONERY OFFICE

1966

SEVEN SHILLINGS NET

U.D.C. No. 533.693.3 : 533.6.013.413 : 533.6.013.42

C.P. No.845

June 1962

THE LATERAL OSCILLATION OF SLENDER AIRCRAFT

by

A. J. Ross, Ph.D.

SUMMARY

Theoretical estimates of the angle of incidence at which the damping of the Dutch-roll oscillation of various slender-wing configurations becomes zero are derived and shown to agree well with the critical angle of incidence, observed experimentally, at which free-flying models undergo a sustained oscillation.

Some approximations to the frequency and damping of the oscillation are compared with the exact values, with satisfactory agreement. A criterion for critical angle of incidence is obtained, the complexity of which depends mainly on the inertia distribution of the aircraft.

Replaces R.A.E. Report No. Aero 2666 - ARC 24630

LIST OF CONTENTS

LIST OF TABLES

LIST OF ILLUSTRATIONS

LIST OF ILLUSTRATIONS (Contd.)

1 INTRODUCTION

One of the factors which has to be considered in the choice of design for a supersonic transport aircraft is the lateral stability of slender wings at high incidence. Low-speed tests have shown that at some incidence severe lateral oscillations are possible, which set a limit to the landing performance. Such oscillations were first noted by McKinney and Drake[1] in 1948, using small flying models, and it appeared that slender-wing aircraft might become uncontrollable at moderate incidence. Gray repeated these experiments and found that the results were unduly pessimistic. His further tests[2] showed that the critical angle of incidence at which the lateral oscillations became undamped on a wing with span/length ratio of $\frac{1}{2}$ (with representative inertia distribution) was about 17°, whereas the landing incidence was restricted by other considerations to about 15°.

Gray has subsequently flown various models of differing planform, for which it has been possible to measure the moments of inertia, and to estimate the aerodynamic derivatives, so that comparisons could be made between experimental and theoretical results. These results, described in the present report, show that the onset of critical conditions can be adequately predicted using the linearized lateral equations of motion. The theoretical angle of incidence at which zero damping of the classical Dutch roll oscillation occurs correlates well with Gray's "cross-over points", i.e. the angle of incidence at which the oscillation is observed to have zero damping. Similar good agreement is found between the theory and Bisgood's tests on larger free-flying models.

It may be noted that it is not necessary to invoke marked changes of aerodynamic characteristics, such as might be associated with vortex breakdown, in order to explain the phenomenon of zero damping. The damping-in-yaw, n_r, is the only derivative showing large variation with incidence, and although the loss in damping-in-yaw does contribute to the loss in damping of the lateral oscillation, it is shown to be by no means the major factor.

Some approximations for the frequency and damping of the Dutch roll oscillation have also been considered. With a slight modification to account for the present large products of inertia at large incidence (referred to the wind-body system of axes), the approximations given by Thomas and Neumark[3], based on an algebraic iterative solution of the lateral stability quartic, are found to be applicable to slender-wing aircraft with reasonable accuracy. Further approximations are made to the expression for the damping, in order to find criteria for the critical angle of incidence. When the inertia in roll is small, and inertia in yaw large, the criterion is of a simple form, and ultimately reduces to that given by Pinsker[4], but as the inertia in roll becomes larger than about 0·1, or the inertia in yaw less than about 1·0, additional terms have to be considered for satisfactory agreement with the exact theory.

These approximations are used as a basis for discussing the relative importance of the rotary derivatives on the damping, and to show how their variation with incidence causes the damping to be reduced. The influence of the inertia distribution is also discussed briefly.

2 EQUATIONS OF MOTION

The linearized equations for the lateral motion, referred to the wind-body system of axes, are[3]:-

$$
\left.
\begin{aligned}
(D - y_v)\,\hat{v} + \hat{r} - \tfrac{1}{2} C_L \varphi &= \tfrac{1}{2} C_y \\
-\mu_2 \frac{\ell_v}{i'_A}\,\hat{v} + \left(D - \frac{\ell_p}{i'_A}\right)\hat{p} - \left(\frac{i'_E}{i'_A} D + \frac{\ell_r}{i'_A}\right)\hat{r} &= \frac{\mu_2}{i'_A} C_\ell \\
-\mu_2 \frac{n_v}{i'_C}\,\hat{v} - \left(\frac{i'_E}{i'_C} D + \frac{n_p}{i'_C}\right)\hat{p} + \left(D - \frac{n_r}{i'_C}\right)\hat{r} &= \frac{\mu_2}{i'_C} C_n \\
-\hat{p} - \tan\gamma_e\,\hat{r} + D\varphi &= 0 \\
-\sec\gamma_e\,\hat{r} + D\psi &= 0
\end{aligned}
\right\} \quad (1)
$$

where $D \equiv \frac{d}{d\tau}$, τ being aerodynamic time.

These equations lead to the well-known stability quartic, which usually has two real roots (the roll subsidence, and spiral root) and a pair of complex roots (Dutch-roll oscillation). If the factors of the stability quartic are written as

$$(D + \lambda_1)\,(D + \lambda_2)\,(D^2 + 2RD + R^2 + J^2)\ ,$$

then the response of the aircraft to any lateral disturbances such as application of aileron, or a side gust, will take the form,(see e.g. Ref.5) for the linear and angular velocities,

$$\hat{v} = \hat{v}_1 + \hat{v}_2 e^{-\lambda_1 \tau} + \hat{v}_3 e^{-\lambda_2 \tau} + (\hat{v}_4 \cos J\tau + \hat{v}_5 \sin J\tau)\, e^{-R\tau}$$

$$\hat{p} = \hat{p}_1 + \hat{p}_2 e^{-\lambda_1 \tau} + \hat{p}_3 e^{-\lambda_2 \tau} + (\hat{p}_4 \cos J\tau + \hat{p}_5 \sin J\tau)\, e^{-R\tau}$$

$$\hat{r} = \hat{r}_1 + \hat{r}_2 e^{-\lambda_1 \tau} + \hat{r}_3 e^{-\lambda_2 \tau} + (\hat{r}_4 \cos J\tau + \hat{r}_5 \sin J\tau)\, e^{-R\tau}\ .$$

The constants $\hat{v}_1$, $\hat{v}_2$ ... $\hat{p}_1$ ... $\hat{r}_5$, are dependent on the initial conditions of the motion, and the applied forces and moments,so that the various terms become dominant for different types of disturbances. As $\tau \to \infty$, the aircraft tends to a new equilibrium condition, $\hat{v} \to \hat{v}_1$, $\hat{p} \to \hat{p}_1$, $\hat{r} \to \hat{r}_1$, if λ_1, λ_2 and R are positive, but diverges if any one of λ_1,λ_2 or R is negative. The roll subsidence root, λ_1 say, is usually large and positive, and as its name implies, is associated with the rolling motion of the aircraft. The spiral root, λ_2, is found to be small, and can in practice be slightly negative without causing intolerable control demands. The oscillation, which is the main interest of the present paper, is usually of moderate or short period, and may be damped or divergent. When the damping R does fall below zero, so that the diverging response attains large amplitudes, non-linear terms neglected in the stability analysis become important, and in practice an oscillation of limited large amplitude is often observed. For

satisfactory handling an aircraft requires a margin of positive damping, and the specification in A.P.970 for damping to frequency ratio is that the number of cycles to half amplitude should be less than 1.

With such a complicated system of equations, it is difficult to interpret physically the part each derivative plays in the various modes. Pinsker, in a recent paper[4], has discussed the kinematics of the lateral motion, and has been able to illustrate the separate modes showing the orientation of the aircraft along its flight path, with the principal forces and moments acting on it. Another approach is to obtain approximations for the dampings and frequency as algebraic expressions involving the derivatives and inertias. Pinsker[4] and Thomas[3,6] have derived formulae which apply to different types of aircraft, and these demonstrate how the importance of a particular derivative may change with the configurations; for example, damping-in-roll (ℓ_p) contributes little to the damping of the Dutch-roll oscillation for aircraft with unswept, large-aspect-ratio wings, but is the major term in the formula appropriate to slender-wing aircraft. These approximations, and their implications for slender-wing aircraft, are discussed more fully in section 4.

For the comparison of the results from theory and experiment, the roots of the stability quartics were evaluated exactly, and the results are shown as the variation of the damping expressed as the logarithmic decrement, with incidence for each case considered.

3 COMPARISON OF THEORETICAL AND EXPERIMENTAL RESULTS

The free-flying model technique has been used extensively by W.E. Gray, in order to assess the angle of incidence at which slender wing aircraft tend to become unstable. The models were launched by hand or catapult, the trimmed angle of incidence being increased until a sustained oscillation was observed. The critical angle of incidence was deduced from photographic records. Various series of tests were undertaken, one of the earliest being to investigate the effect of span/length ratio, and these experimental results are shown in Fig.1. No attempt has been made to calculate the corresponding theoretical values, due to the lack of aerodynamic data on the narrowest shape. Later tests by Gray were carried out in conjunction with the theoretical work, and the experimental results (as yet unpublished), were put at our disposal. The comparison with the theoretical results is discussed in the following sections 3.1 to 3.3 for various models. In section 3.4 the experimental and theoretical results for Bisgood's models[7] (which are of larger scale than Gray's) are given.

3.1 Simple model

The basic comparison between theory and experiment was for a model consisting of a delta wing with rounded tips, span/length ratio of $\frac{1}{2}$, and a 60° delta fin of 10% of the wing area. The centre line chord of the model was 13 in. and the wing (which was carved from plastic foam, and weighed only 0·4 ounce) was ballasted to give the correct weight, about 1·2 ounces, for dynamic similarity to a full scale aircraft ($\mu_2 = 13{\cdot}9$), and to adjust the moments of inertia. The model was flown with two different mass distributions, one to give $i_{C_o} = 1{\cdot}0$, $i_{A_o} = 0{\cdot}1$ (centre of gravity at 0·51 c_o) and the second to give $i_{C_o} = 1{\cdot}0$, $i_{A_o} = 0{\cdot}2$ (centre of gravity at 0·535 c_o).

The variation of the derivatives with incidence as assumed for this model is shown in Fig.2, and the sources of information are given in Table 1. Experimental results (as available at the time of the calculations, early in 1959) were used for the sideslip and rolling derivatives, although the fin

effect on the sideslip derivatives had to be estimated. Subsequent experimental results have not shown any appreciable changes, and have confirmed the value assumed for the damping-in-yaw. However, the value of the rolling moment due to yaw, ℓ_r, still remains uncertain.

The theoretical results for the logarithmic decrement, and the experimental "cross-over" points found by Gray, are shown in Fig.3. For both models, the estimated angle of incidence for zero damping is about 2·5° higher than the experimental value, for the basic calculations with the principal axis of inertia inclined at -1° to the root chord, and with the flight path angle observed in the experiments ($\tan \gamma_e = -0{\cdot}25$). From Fig.3a, it is seen that level flight would be slightly more stable. The calculations were also repeated for an increased angle of inclination of the principal axis of inertia ($\varepsilon = -3°$). This made little difference to the logarithmic decrement of the model with $i_{A_o} = 0{\cdot}1$ at high incidences and the angle of incidence for zero damping was hardly affected. For the model with $i_{A_o} = 0{\cdot}2$, the critical angle of incidence is smaller, so that the inclination of the inertia axis has a greater effect, and the theory indicated an increase of $4\frac{1}{2}°$ in the critical angle of incidence when the inclination of the inertia axis varied from -3° to +3°.

3.2 H.P.115 model

The design of the H.P.115 research aircraft, with low cockpit, and engine installed high at the rear, leads to a greater inclination of the principal inertia axis to the no-lift-line than had previously been considered, and so a representative model was tested by Gray. These experiments indicated that in this case there was no appreciable change in the critical angle of incidence for a large range of ε, and some further results have been calculated for comparison. The inertias were taken as $i_{A_o} = 0{\cdot}065$, $i_{C_o} = 0{\cdot}86$, with $\varepsilon = -1°$ and -5°. The derivatives used were those of Fig.2, since the small effects on the values due to the differences in design between the simple model and the H.P.115 could not be estimated accurately.

Although the theory confirms that the critical angle of incidence is approximately the same (see Fig.4a), the logarithmic decrement at the lower incidences is much smaller for $\varepsilon = -5°$ than for $\varepsilon = -1°$. For an extreme value of the inclination of $\varepsilon = -8°$, it was found theoretically that the Dutch-roll oscillation became unstable at low incidences also, and this was confirmed qualitatively by experiment, as shown in Fig.4(b). The inertias evaluated for this model, and used in the calculation, were $i_{A_o} = 0{\cdot}1$, $i_{C_o} = 1{\cdot}2$, and the variation of the inclination of the flight path with incidence was also taken into consideration. The "dip" in the logarithmic decrement curve between $\alpha = 0°$ and $\alpha = 10°$ is probably exaggerated in Figs.4a and b due to the value of ℓ_p assumed in the calculations, which later experimental results showed to be unduly low at the moderate incidences. Calculations using these experimental values of ℓ_p for the wing with $\varepsilon = -8°$, show the order of the change in the logarithmic decrement between the two sets of values of ℓ_p (Fig.4b).

3.3 Ogee wing model

Gray made and tested a model of a possible aircraft design, the wing planform and thickness distribution being that of the uncambered Ogee wing

described in Ref.8, with a triangular fin, and found the critical incidence to be 20°. The derivatives for the design were estimated early in 1960 (before tunnel tests on the actual model were available) from the sources noted in Table 2, and the results are plotted in Fig.5. The Dutch-roll oscillation is well damped (Fig.6) up to moderate incidences, but loses damping rapidly as the angle of incidence increases above 15°, with the critical angle of incidence in the region of 22·5°. This is again a few degrees higher than experiment indicated.

3.4 Bisgood's models

The free-flight models flown by Bisgood[7] were delta wings, of aspect ratio 1·0, with a triangular fin extending behind the trailing edge of the wing. The models were larger than Gray's, having a root chord of 6 ft and weighing about 15 lb. The critical angle of incidence was found for two different inertia ratios, with i_{C_o}/i_{A_o} = 14 and 7·5 (referred to in Ref.7 as the models with pitch/roll inertia ratios of 13 and 7 respectively), for a centre of gravity position at 0·583 c_o for both models. The derivatives for the configuration were estimated from tunnel tests for a triangular fin on a gothic wing, with the assumption that the fin contribution is independent of wing planform, so that the relationships used were:-

(Delta wing + fin) ≡ (delta wing) + (gothic wing + fin) - (gothic wing) .

Corrections had to be made for the shift of centre of gravity, and ℓ_r had to be estimated from slender-wing theory. The calculated derivatives are shown in Fig.7.

The glide path angles, taken as $\tan \gamma_e = -C_D/C_L$, with values of the lift/drag ratio estimated from tunnel tests, was found to have an appreciable effect on the critical incidence: see Fig.8, where the variation of logarithmic decrement with incidence for $\tan \gamma_e = -C_D/C_L$ and $\tan \gamma_e = 0$ is shown. The Dutch-roll oscillation has zero damping at an incidence about 4° higher than the experiments indicated for both models. On the basis of some preliminary wind tunnel results for $\ell_r - \ell_{\dot{v}}$, which indicated a loss in this derivative as incidence increases, an arbitrary reduction was made in ℓ_r, as shown by the dotted curve in Fig.7. This large change in ℓ_r at high angles of incidence leads to a correspondingly large reduction in damping of the Dutch-roll oscillation, and the critical angle of incidence is found to be 1° below the experimental value (Fig.8).

4 APPROXIMATIONS

Since the exact evaluations of the frequency and damping of the Dutch-roll oscillation involves the solution of a quartic, i.e. is of necessity a numerical iterative process, it is desirable to obtain approximate algebraic solutions in order to study the effects of individual parameters. The approximations suggested in Ref.3 have been found to give good agreement with exact values when μ_2, the relative density, is large. However, in deriving the expressions for R and J, the term $e_A e_C$ was neglected compared with unity; for slender-wing aircraft, the product of inertia becomes large at large incidences and so the simple modification to the approximation to include the $e_A e_C$ term is made in the analysis below.

4.1 Frequency of Dutch-roll oscillation

The approximation to the frequency corresponding to eqn.(11) of Ref.3 is

$$J \approx \sqrt{\frac{\omega_n - e_C\omega_\ell}{1 - e_A e_C}} = \sqrt{\frac{\mu_2(i'_A n_v + i'_E \ell_v)}{(i'_A i'_C - i'^2_E)}} \quad . \qquad (2)$$

The correlation of the exact and approximate values of the frequency for the models considered above is shown in Fig.9 and except for a few of the results for the large inertia axis tilt, all approximate values are within ±5% of the exact value. This is better than might have been expected, since μ_2 is not so very large for these configurations, being between 10 and 20, as compared with values between 66 and 702 in Ref.3.

4.2 Damping of Dutch-roll oscillation

With the stability quartic written in the form

$$D^4 + B'D^3 + C'D^2 + D'D + E' = 0 \quad .$$

Thomas and Neumark[3] found that a good approximation to the damping of the lateral oscillation is given by

$$2R \approx B' - \frac{D'}{C'}$$

$$\approx \bar{y}_v + \left\{\frac{\nu_\ell + \nu_n + e_A\nu_{np} - e_C\nu_{\ell r}}{1 - e_A e_C}\right\} - \left\{\frac{\omega_n\nu_\ell + \omega_\ell\nu_{np} + \frac{1}{2}C_L(\omega_\ell - e_A\omega_n)}{\omega_n - e_C\omega_\ell}\right\} \qquad (3)$$

on the assumption that the relative density, μ_2, is large. If the assumption is also made that second-order terms in the product of inertia may be neglected, then eqn.(3) reduces to eqn.(10a) of Ref.3.

In terms of the derivatives and inertias, eqn.(3) may be written as

$$2R \approx -y_v - \frac{\{i'_C\ell_p + i'_A n_r + i'_E n_p + i'_E\ell_r\}}{(i'_A i'_C - i'^2_E)}$$

$$+ \frac{\{n_v\ell_p - \ell_v n_p + \frac{1}{2}C_L(i'_C\ell_v + i'_E n_v)\}}{(i'_A n_v + i'_E\ell_v)} \qquad (3a)$$

Thomas[6] has derived a slightly simpler form for aircraft with $i_C \gg i_A$, and assuming that $i'_E = -i_C \sin\alpha$, which is

$$2R \approx -y_v - \frac{\{\ell_p - (n_p + \ell_r - \ell_{\dot{v}}) \sin\alpha\}}{i_A - i_C \sin^2\alpha} - \frac{1}{\sin\alpha}\left(\frac{C_L}{2} - \frac{n_p}{i_C}\right) + \frac{1}{2}\frac{n_v}{\ell_v} C_L$$

but this approximation has not been checked with exact values*.

When the flight path is inclined to the horizontal, additional terms appear in the coefficients of the stability quartic to those considered in Ref.3, and a better approximation to the damping is given by adding the term $\frac{1}{2} C_L \tan\gamma_e$ to the right hand side of equation (3)(or (3a)).

The comparison between the approximations (with and without the 'tan γ_e' term) and the exact value is shown in Figs.10 (a and b) for the models discussed in sections 3.1 and 3.4. The agreement is again good, and the critical angle of incidence is given to within $\pm\frac{1}{2}^\circ$ for three of the configurations, there being a 2° discrepancy for the model with low inertia in yaw**.

The variation of the damping with the rotary derivatives is also satisfactorily given by the approximation (3). Partial differentiation yields:-

---

* It may be noted that in the analysis of this report the derivative $\ell_{\dot{v}}$ has been assumed to have a negligible effect on the motion, although in the proposed approximations $\ell_{\dot{v}}$ may be considered to be combined with ℓ_r, i.e. ℓ_r is replaced by $\ell_r - \ell_{\dot{v}}$.

** In these calculations for Bisgood's configurations, the theoretical value of ℓ_r has been used, and not the reduced ℓ_r considered in the exact solution to the stability quartic (section 3.4).

$$\frac{\partial R}{\partial \ell_p} \approx \frac{e_C}{2i'_A}\left\{\frac{\omega_\ell - e_A\omega_n}{\omega_n - e_C\omega_\ell}\right\}\frac{1}{(1 - e_Ae_C)}$$

$$= -\frac{i'_E}{2(i'_Ai'_C - i'^2_E)}\left\{\frac{i'_C\ell_v + i'_En_v}{i'_An_v + i'_E\ell_v}\right\} \qquad (4)$$

$$\frac{\partial R}{\partial n_p} \approx \frac{1}{2i'_C}\left\{\frac{\omega_\ell - e_A\omega_n}{\omega_n - e_C\omega_\ell}\right\}\frac{1}{(1 - e_Ae_C)}$$

$$= -\frac{i'_A}{2(i'_Ai'_C - i'^2_E)}\left\{\frac{i'_C\ell_v + i'_En_v}{i'_An_v + i'_E\ell_v}\right\} \qquad (5)$$

$$\frac{\partial R}{\partial \ell_r} \approx -\frac{e_C}{2i'_A(1 - e_Ae_C)} = -\frac{i'_E}{2(i'_Ai'_C - i'^2_E)} \qquad (6)$$

$$\frac{\partial R}{\partial n_r} \approx -\frac{1}{2i'_C(1 - e_Ae_C)} = \frac{-i'_A}{2(i'_Ai'_C - i'^2_E)}\,. \qquad (7)$$

Some results are shown in Fig.11, where the exact and approximate slopes have both been drawn through the exact values of the damping at the datum value of the derivative. These calculations were based on an earlier set of derivatives and inertias, in which n_p was taken from tunnel tests on a model without fin, so that the n_p variation is unrepresentative (a fin makes n_p large in the negative sense). The approximation has been checked for a more realistic variation of n_p.

Typical values of the slopes, evaluated for the model with $i_{A_o} = 0{\cdot}1$, $i_{C_o} = 1{\cdot}0$, at $C_L = 0{\cdot}6$ are:-

$$\frac{\partial R}{\partial \ell_p} = -3{\cdot}36, \quad \frac{\partial R}{\partial n_p} = 2{\cdot}39, \quad \frac{\partial R}{\partial \ell_r} = 1{\cdot}25, \quad \frac{\partial R}{\partial n_r} = -0{\cdot}89\,,$$

and the variation of the slopes with incidence for this model, and for one of Bisgood's[7], is shown in Fig.12. It may be seen that changes in the derivatives due to rolling, ℓ_p and n_p, have more than twice the effect of the same incremental change in the derivatives due to yawing, ℓ_r and n_r.

The variation of the damping with the inertias is not so readily given, and the formulae are too complicated to be useful, even if expressed with the derivatives and inertias referred to the principal inertia axes (see equation 8).

4.3 Critical incidence

As equation (3) stands, the derivatives, inertia terms and C_L are all dependent on the angle of incidence and so, in order to simplify the analysis, the expression has been transformed so that the derivatives and inertias are referred to the principal inertia axes, denoted by subscript '0'. i_{A_o} and i_{C_o} are now of course independent of α, and equation (3) (plus the flight path angle term $\frac{1}{2} C_L \tan \gamma_e$) becomes

$$2R \approx -y_v + \tfrac{1}{2} C_L \tan \gamma_e + \frac{1}{\left(1 + \frac{n_{v_o}}{\ell_{v_o}} \frac{i_{A_o}}{i_{C_o}} \cot e\right)} \left\{ -\frac{\ell_{p_o}}{i_{A_o}} - \frac{n_{p_o}}{i_{C_o}} \cot e - \frac{n_{v_o}}{\ell_{v_o}} \frac{\ell_{r_o}}{i_{C_o}} - \frac{n_{v_o}}{\ell_{v_o}} \frac{n_{r_o}}{i_{C_o}} \frac{i_{A_o}}{i_{C_o}} \cot e + \tfrac{1}{2} C_L \cot e \left(1 - \frac{n_{v_o}}{\ell_{v_o}} \frac{i_{A_o}}{i_{C_o}} \tan e\right)\right\}, \quad (8)$$

where $e = -\alpha - \varepsilon$, and ε is the inclination of the principal inertia axis to the no-lift line. The first two terms are small, and often of opposite sign, and so R is approximately proportional to the expression inside the curly brackets. If we also assume $i_{A_o} << i_{C_o}$, so that $i_{A_o}/i_{C_o} \tan e$ is small, then, approximately

$$R \propto \left\{ -\frac{\ell_{p_o}}{i_{A_o}} + \frac{n_{p_o}}{i_{C_o}} \cot(\alpha+\varepsilon) - \frac{n_{v_o}}{\ell_{v_o}} \frac{\ell_{r_o}}{i_{C_o}} + \frac{n_{v_o}}{\ell_{v_o}} \frac{n_{r_o}}{i_{C_o}} \frac{i_{A_o}}{i_{C_o}} \cot(\alpha+\varepsilon) - \tfrac{1}{2} C_L \cot(\alpha+\varepsilon) \right\} \quad (9)$$

The dominant terms are $-\frac{\ell_{p_o}}{i_{A_o}}$ and $-\frac{1}{2} C_L \cot(\alpha+\varepsilon)$, which, being of the same order but of opposite sign, tend to cancel each other. Thus, the damping, R, will be very small if

$$\tfrac{1}{2} C_L \cot(\alpha + \varepsilon) = -\frac{\ell_{p_o}}{i_{A_o}} . \quad (10)$$

This is similar to the condition given by Pinsker[4] (equation 47) that the motion is unstable if

$$\tfrac{1}{2} C_L \operatorname{cosec}(\alpha + \varepsilon) > -\frac{\ell_{p_o}}{i_{A_o}} .$$

However, this simple formula does not adequately define the critical angle of incidence, since the smaller terms became significant when eqn.(10) is approximately satisfied. This is illustrated in Figs.13(a and b) where the functions $\frac{1}{2} C_L \cot(\alpha + \varepsilon)$

$$f_1 = -\ell_{p_o}/i_{A_o}$$

$$f_2 = -\ell_{p_o}/i_{A_o} + \frac{n_{p_o}}{i_{C_o}} \cot(\alpha + \varepsilon)$$

$$f_3 = -\ell_{p_o}/i_{A_o} + \frac{n_{p_o}}{i_{C_o}} \cot(\alpha + \varepsilon) - \frac{n_{v_o}}{\ell_{v_o}} \frac{\ell_{r_o}}{i_{C_o}}$$

$$f_4 = -\ell_{p_o}/i_{A_o} + \frac{n_{p_o}}{i_{C_o}} \cot(\alpha + \varepsilon) - \frac{n_{v_o}}{\ell_{v_o}} \frac{\ell_{r_o}}{i_{C_o}} + \frac{n_{v_o}}{\ell_{v_o}} \frac{n_{r_o}}{i_{C_o}} \frac{i_{A_o}}{i_{C_o}} \cot(\alpha + \varepsilon)$$

are plotted against α. R will be very small (of order of neglected terms) in the regions of the intersections of the functions f_1 to f_4 with the $\frac{1}{2} C_L \cot(\alpha + \varepsilon)$ curve, so that these intersections give approximations to the value of the critical angle of incidence. The exact value is also marked on the $\frac{1}{2} C_L \cot(\alpha + \varepsilon)$ curve, for comparison.

The relative importance of the smaller terms in equation (9) is seen to differ for the different inertia distributions considered. Even for i_{A_o} small and i_{C_o} large, the destabilising term, $n_{p_o}/i_{C_o} \cot(\alpha + \varepsilon)$, is significant, and

$$\frac{1}{2} C_L \cot(\alpha + \varepsilon) = f_2$$

gives a good approximation for the critical angle of incidence, as shown in Fig.13a, upper diagram, and Fig.13b, lower diagram. For the larger i_{A_o} (= 0·2) the term containing $n_{r_o} i_{A_o}/i_{C_o}$ is larger, and the functions f_1 to f_3, which neglect this term, indicate negative damping in the incidence range considered (Fig.13b). Inclusion of this stabilising n_r term in f_4 leads to a slightly pessimistic value of critical angle of incidence, 15°, compared with the exact value of 17·5°. The function f_4 has also to be considered for the configuration with smaller inertia in yaw, i_{C_o} = 0·82.

For some of the current proposed designs, the estimated i_{A_o} is of the order of 0·1 with i_{C_o} greater than 1·0, and so the criterion

$$\frac{1}{2} C_L \cot(\alpha + \varepsilon) = -\frac{\ell_{p_o}}{i_{A_o}} + \frac{n_{p_o}}{i_{C_o}} \cot(\alpha + \varepsilon) \qquad (11)$$

for critical angle of incidence should be applicable. Unfortunately it is not possible to express the derivatives due to rolling solely in terms of planform parameters and incidence, since the sidewash on the fin due to

the rolling wing contributes large moments on the aircraft. It should also be noted that most experimental results for rotary derivatives are quoted with respect to wind-body axes, so that derivatives due to yawing must also be known in order to estimate ℓ_{p_o} and n_{p_o}, since

$$\left.\begin{aligned} \ell_{p_o} &= \ell_p \cos^2\delta - (\ell_r + n_p) \cos\delta \sin\delta + n_r \sin^2\delta \\ n_{p_o} &= n_p \cos^2\delta - (n_r - \ell_p) \cos\delta \sin\delta - \ell_r \sin^2\delta \end{aligned}\right\} \quad (12)$$

where ℓ_p, n_p, ℓ_r and n_r are measured with respect to axes inclined at an angle δ to the principal inertia axes (δ positive if principal inertia x_o-axis is below reference x-axis). Thus, for the usual transformation from wind-body to principal inertia axes, $\delta = \alpha + \varepsilon$, and ℓ_{p_o} and n_{p_o} are functions of α and ε*.

The derivatives shown in Figs.2 and 7 for Gray's and Bisgood's models respectively have been transformed to the principal inertia axes with $\varepsilon = -1^\circ$, the results being shown in Fig.14. The variation of the derivatives with incidence is seen to be similar for both systems of axes, and also for both configurations, although the magnitudes are slightly different. The one exception is ℓ_r, where for Bisgood's configuration the slender-body value was assumed, but for Gray's configurations an attempt was made to relate the loss in damping-in-yaw found experimentally on a wing-alone model to a loss in the rolling moment, assuming that both moments are due to the normal force alone, so that $\ell_r \approx -n_r \tan\alpha$. Some preliminary results from tunnel tests, by Thompson and Owen at the R.A.E., for the combined derivative $\ell_r - \ell_v$ for various slender wings do not establish any obviously definite trends.

In the region of the critical angle of incidence, i.e. above about 17°, it may be seen that the magnitudes of y_v, ℓ_p and n_r decrease with increasing incidence, while n_p increases negatively, and these trends all contribute to the loss in damping of the lateral oscillation (see e.g. equ.8). The decreasing ℓ_r assumed for Gray's models also acts in this way, as shown by the difference between the f_2 and f_3 curves in Fig.13a, but the increasing value of ℓ_r assumed for Bisgood's models makes the term $\frac{n_{v_o}}{\ell_{v_o}} \frac{\ell_{r_o}}{i_{C_o}}$ included in f_3 a nearly constant positive part of the damping (Fig.13b). Another point of interest is that in the calculations for the model with $i_{A_o} = 0{\cdot}2$, $i_{C_o} = 1{\cdot}0$, where the critical angle of incidence is lower, the ℓ_p term contributes an increasing amount to the lateral damping as the incidence increases up to the critical value (f_1 in Fig.13a, lower diagram) and it is the variation of y_v, n_p, ℓ_r and n_r with incidence which leads to the increased rate of reduction of R to zero.

---

* Wind tunnel techniques are now in use which could be used to measure the moments for models oscillating about any body axis.

Although the above discussion demonstrates how the damping decreases in terms of the variation of the derivatives with incidence, it still remains to explain why the derivatives vary as they do. It has been shown[6] that the trends of the derivatives due to rolling can be predicted theoretically, using slender-body theory with corrections for sidewash effects on the fin, though a complete analysis accounting for the asymmetry in the strength and position of the leading edge vortices would be needed to obtain results in more exact quantitative agreement with experiment. As has been mentioned previously, the experimental results for damping-in-yaw indicated a marked loss in damping as the incidence increases, but no satisfactory explanation, which could be checked theoretically, has yet been given.

It should be noted that the models considered in this report are of relatively simple design, and modifications to the derivatives due to the effect, for example, of a body or of wing camber, may alter the dynamics of the aircraft considerably. The theoretical estimation of such effects is difficult, especially when the wing is at incidence, and so it is not possible at present to predict whether any such changes to the designs would be detrimental or beneficial as regards the damping of the lateral oscillation.

Some general conclusions may be drawn as to the effect of different inertia distributions on the same wing-fin configurations. The critical angle of incidence will obviously be higher if the inertia in roll is designed to be as small as possible, so that the damping-in-roll term, $-\frac{\ell_{p_o}}{i_{A_o}}$, becomes more effective. Increasing the inertia in yaw will also decrease the destabilising effect of the $\frac{n_{p_o}}{i_{C_o}} \cot(\alpha + \varepsilon)$ term, and so the ideal inertia distribution, from the lateral stability point of view, is to have the majority of the mass along the centre line. It is also desirable to keep the principal inertia axis as near to the no-lift-line as possible (the presence of the fin usually prevents ε from being positive, which would be the most advantageous). If the critical angle of incidence is reasonably high, variation of ε within a few degrees would not be significant, since the relevant parameter is $(\alpha + \varepsilon)$, but it should be remembered that the damping at lower incidences is decreased if ε increases negatively (e.g. Fig.4). At very low incidences, $\alpha + \varepsilon \approx 0$, and eqn.(8) reduces to the more familiar approximation,

$$2R \approx - y_v - \frac{n_{r_o}}{i_{C_o}} , \qquad (13)$$

(since n_{p_o}, ℓ_{v_o} and C_L are now small), and is again not very dependent on ε.

5 CONCLUSIONS

The critical angle of incidence at which free-flight models of slender aircraft are observed to become unstable has been shown to correlate with the incidence at which the damping of the Dutch-roll oscillation is theoretically zero. The theory uses the linearized equations of motion, with derivatives estimated from available tunnel data and slender-body theory. Comparisons have been made between the experimental results obtained by Gray[2] and Bisgood[7], with the theoretical results for various models, on which the inertias and inclination of the principal inertia axis have been varied.

The approximations for the frequency and damping of the Dutch-roll oscillation proposed by Thomas and Neumark[2], when slightly modified to retain the product of inertia term, i_E^2, as in eqns.(2) and (3), are found to give values in good agreement with the exact results, and the variation of the damping with the rotary derivatives is also satisfactorily given in terms of inertias and sideslip derivatives.

A criterion for the critical angle of incidence for aircraft with low inertia in roll is derived, (eqn.11), involving the angle of incidence, lift coefficient, inclination of the principal inertia axis, and the moment derivatives due to rolling about the longitudinal principal inertia axis. For aircraft with the moment of inertia in roll of the order of 0·2, or with inertia in yaw smaller than 1·0, further terms involving the sideslip and yawing derivatives are required to give satisfactory agreement with the exact result, as in eqn.(9).

These successive approximations for the damping, are used to demonstrate how the reduction in magnitude of y_v, ℓ_p and n_r, and the increase in magnitude of n_p with increasing incidence all contribute to the loss in damping of the lateral oscillation. Since the variation of the rotary derivatives with incidence is largely dependent on the sidewash on the fin, no conclusions as to optimum wing/fin planform shapes for high critical angles of incidence can be given. For guidance in the choice of mass distribution, however, it is easily seen that the damping increases as the moment of inertia in roll decreases, and as the moment of inertia in yaw increases. When the inertias are such that the critical angle of incidence is reasonably high, it is shown that the inclination of the principal inertia axis has little effect on the actual value of the critical angle of incidence, but the damping at moderate incidences is reduced if the principal inertia axis lies increasingly below the no-lift line.

ACKNOWLEDGEMENT

The author wishes to thank Mr. W.E. Gray for allowing his experimental results to be quoted, and to acknowledge the guidance given by Mr. H.H.B.M. Thomas throughout the work. Miss F.M. Ward and Mrs.G.Helyer helped with the computations.

LIST OF SYMBOLS

b span of wing

c_o centre line chord of wing

C_ℓ rolling moment/$\frac{1}{2}\rho V^2 Sb$

C_n yawing moment/$\frac{1}{2}\rho V^2 Sb$

C_y sideforce/$\frac{1}{2}\rho V^2 S$

C_L lift/$\frac{1}{2}\rho V^2 S$

e $-\alpha-\varepsilon$

e_A i'_E/i'_A

LIST OF SYMBOLS (Contd.)

e_C	i'_E/i'_C
f_1, f_2, f_3, f_4	functions contributing to damping
i_A	moment of inertia in roll/ms^2
i_C	moment of inertia in yaw/ms^2
i_E	product of inertia/ms^2
J	imaginary part of root of stability quartic
ℓ_p	$\partial C_\ell / \partial \left(\frac{pb}{2V}\right)$
ℓ_r	$\partial C_\ell / \partial \left(\frac{rb}{2V}\right)$
ℓ_v	$\partial C_\ell / \partial \left(\frac{v}{V}\right)$
m	mass of aircraft
n_p	$\partial C_n / \partial \left(\frac{pb}{2V}\right)$
n_r	$\partial C_n / \partial \left(\frac{rb}{2V}\right)$
n_v	$\partial C_n / \partial \left(\frac{v}{V}\right)$
p	rate of roll
$\hat{p}$	$p\hat{t}$
r	rate of yaw
$\hat{r}$	$r\hat{t}$
R	negative of real part of root of stability quartic
s	semi-span of wing
S	wing area
$\hat{t}$	$\frac{m}{\rho S V}$, aerodynamic unit of time
v	sideslip velocity
$\hat{v}$	v/V

LIST OF SYMBOLS (Contd.)

V	aircraft velocity
y_v	$\frac{1}{2}\,\partial C_y / \partial \left(\frac{v}{V}\right)$
α	angle of incidence
γ_e	flight path angle, relative to horizontal
δ	angle between reference axis and principal inertia axis
ε	inclination of principal inertia axis to no-lift axis (positive if principal inertia axis lies above no-lift axis)
λ_1, λ_2	negative of real roots of stability quartic
μ_2	$m/\rho Ss$, relative density
ν_ℓ	$-\ell_p / i'_A$
ν_n	$-n_r / i'_C$
$\nu_{\ell r}$	ℓ_r / i'_A
ν_{np}	$-n_p / i'_C$
ρ	density of air
τ	$\frac{t}{\hat{t}}$, aerodynamic time
φ	angle of bank
ψ	angle of yaw
ω_ℓ	$-\mu_2 \ell_v / i'_A$
ω_n	$\mu_2 n_v / i'_C$

Subscript 'o' refers to principal inertia axes system

Dash ' refers to wind-body axes system

LIST OF REFERENCES

No.	Author(s)	Title, etc.
1	McKinney, M.O. Drake, H.M.	Flight characteristics at low speed of delta-wing aircraft. NACA TIB 1537 1948
2	Gray, W.E.	Unpublished M.o.A. Report
3	Thomas, H.H.B.M. Neumark, S.	Interim note on stability and response characteristics of supersonic aircraft (linear theory) R.A.E. T.N. Aero 2412 ARC 18263 1955
4	Pinsker, W.J.G.	The lateral motion of aircraft, and in particular of inertially slender configurations. ARC R & M 3334 September 1961
5	Neumark, S.	Operational formulae for response calculations. ARC R & M 3075 June 1956
6	Thomas, H.H.B.M.	Estimation of stability derivatives (State of the art) AGARD Report 339 ARC C.P.664 August 1961
7	Bisgood, P.L.	Low-speed investigations using free-flight models. R.A.E. T.N. Aero 2713. ARC 22459 1960
8	Taylor, C.R.	Measurements, at Mach numbers up to 2·8, of the longitudinal characteristics of one plane and three cambered slender "ogee" wings. R.A.E. Rep. Aero 2658. ARC 23776 1961

TABLE 1

Sources of information on derivatives for Gray's simple models

Derivatives	Source of information		Refs.
	Wing contribution	Fin contribution	
y_v	R.A.E. experiments	wing assumed to be complete reflection surface for fin	6
ℓ_v	R.A.E. experiments		
n_v	R.A.E. experiments		
ℓ_r	Slender wing theory modified by experiment		6
n_r	$-\ell_r \tan \alpha$		
ℓ_p	Gray's experiments	Gray's experiments	2
n_p	Gray's experiments	Gray's experiments	
C_L	R.A.E. experiments		

TABLE 2

Sources of information on derivatives for Ogee wing model

Derivatives	Source of information		Refs.
	Wing contribution	Fin contribution	
y_v	$y_v = \frac{1}{2} n_v$	wing assumed to be complete reflection surface for fin	6
ℓ_v	wing plus body contribution from slender body theory		
n_v			
ℓ_r	Slender body theory	Ditto, modified to give loss in damping at high incidences	6
n_r			
ℓ_p	Experimental tests with 10% fin on gothic wing, A.R. = 0·75, corrected for c.g. position		6
n_p			

Note The method of estimation used for the sideslip derivatives have since been checked with experimental results, showing reasonable agreement.

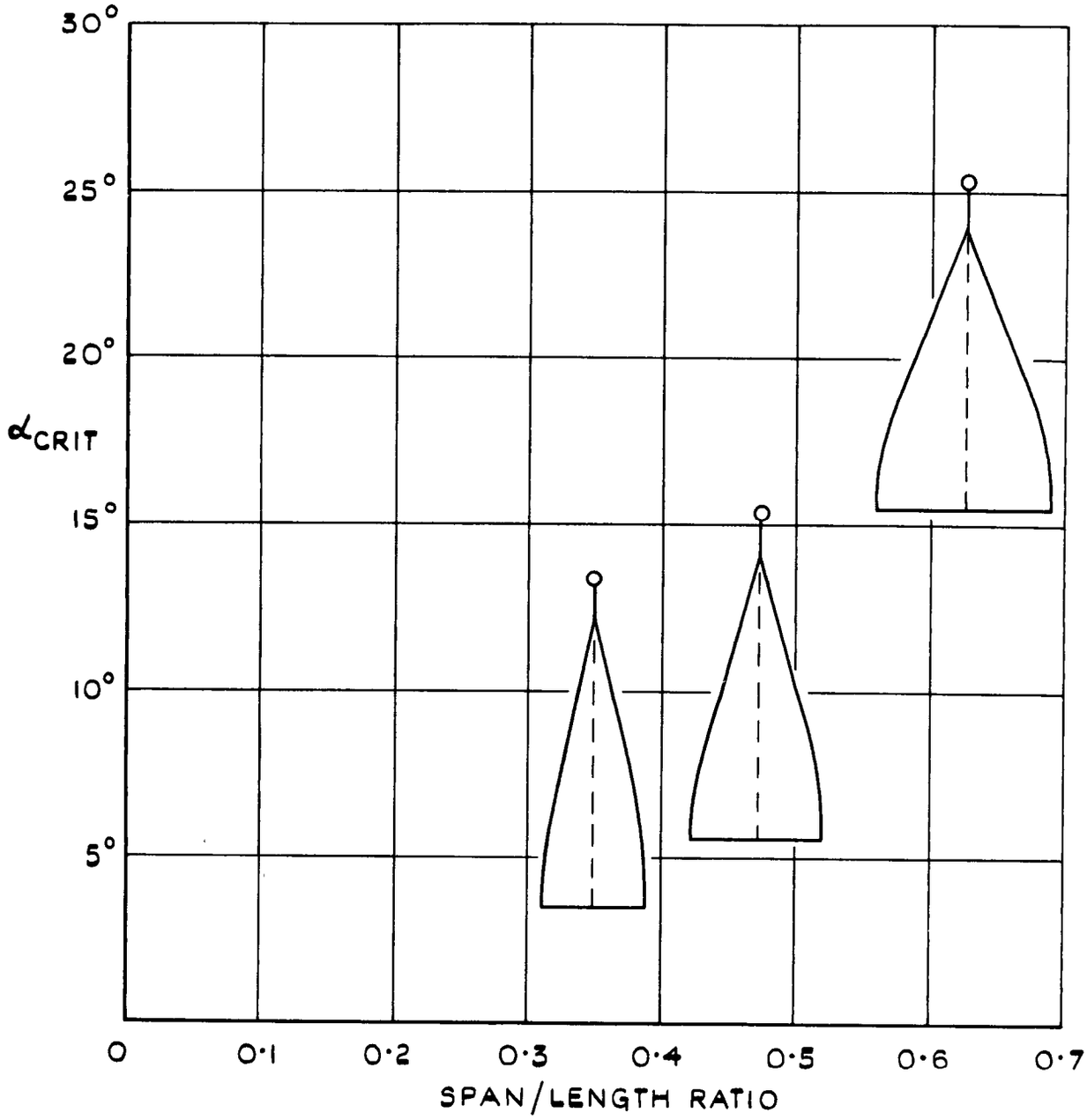

FIG. 1. GRAY'S EXPERIMENTAL RESULTS FOR CRITICAL ANGLE OF INCIDENCE.

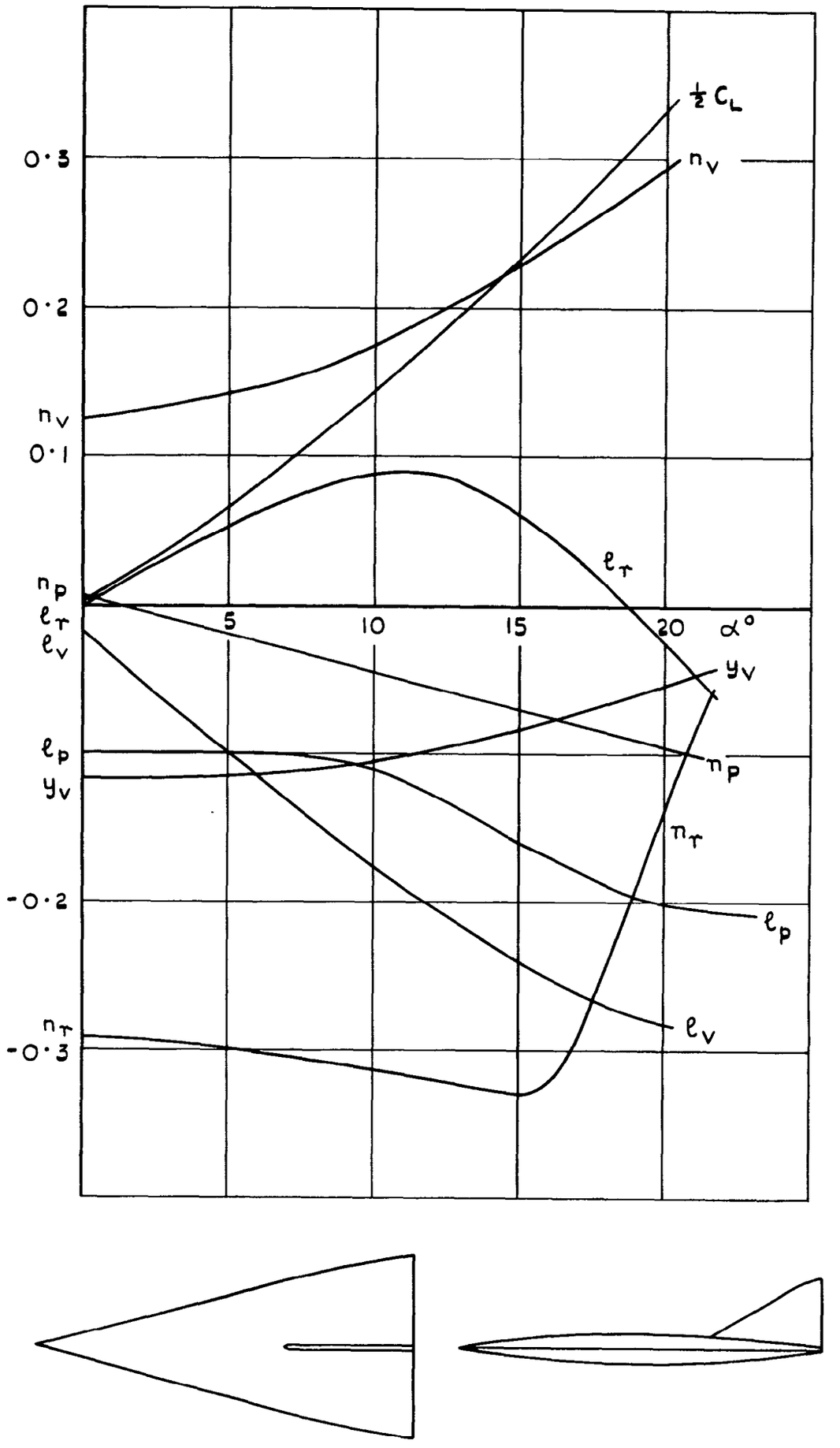

FIG. 2. DERIVATIVES FOR GRAY'S SIMPLE MODELS (REFERRED TO ORIGIN AT 0·593 c_0)

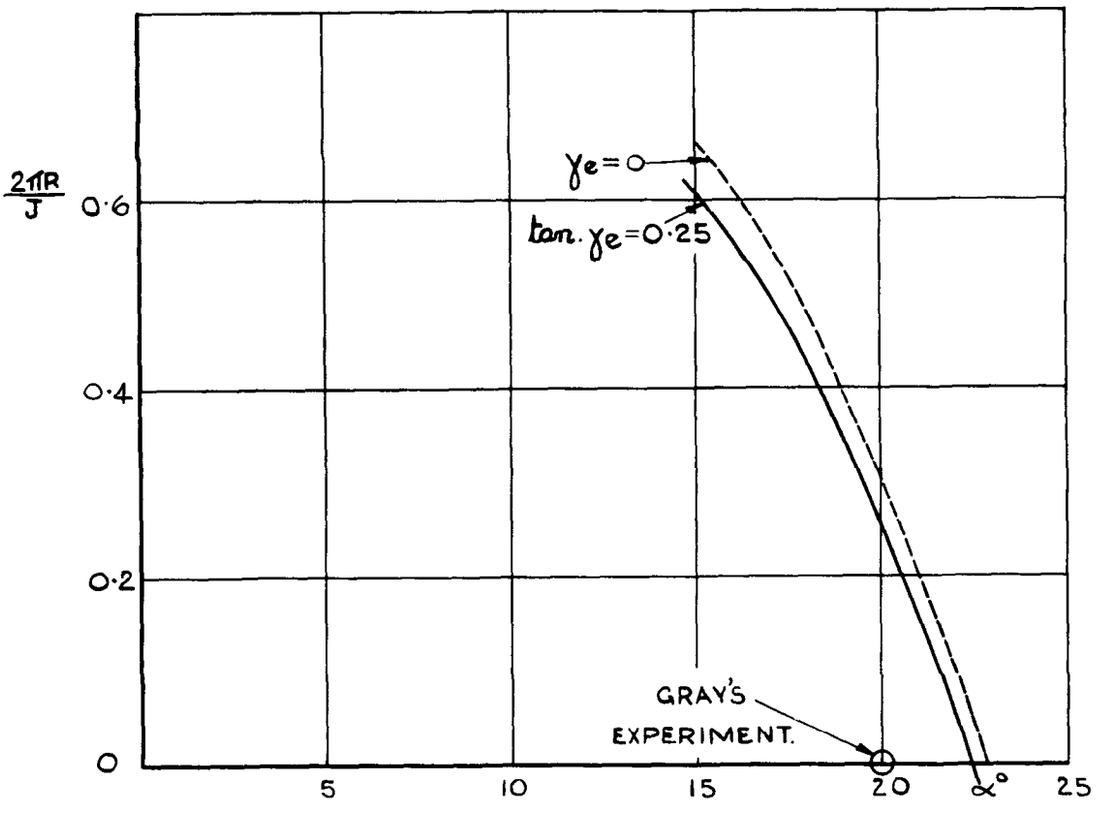

(a.) $i_{c_0} = 1{\cdot}0$, $i_{A_0} = 0{\cdot}1$, $\varepsilon = -1°$

C.G. AT $0{\cdot}51\, c_0$

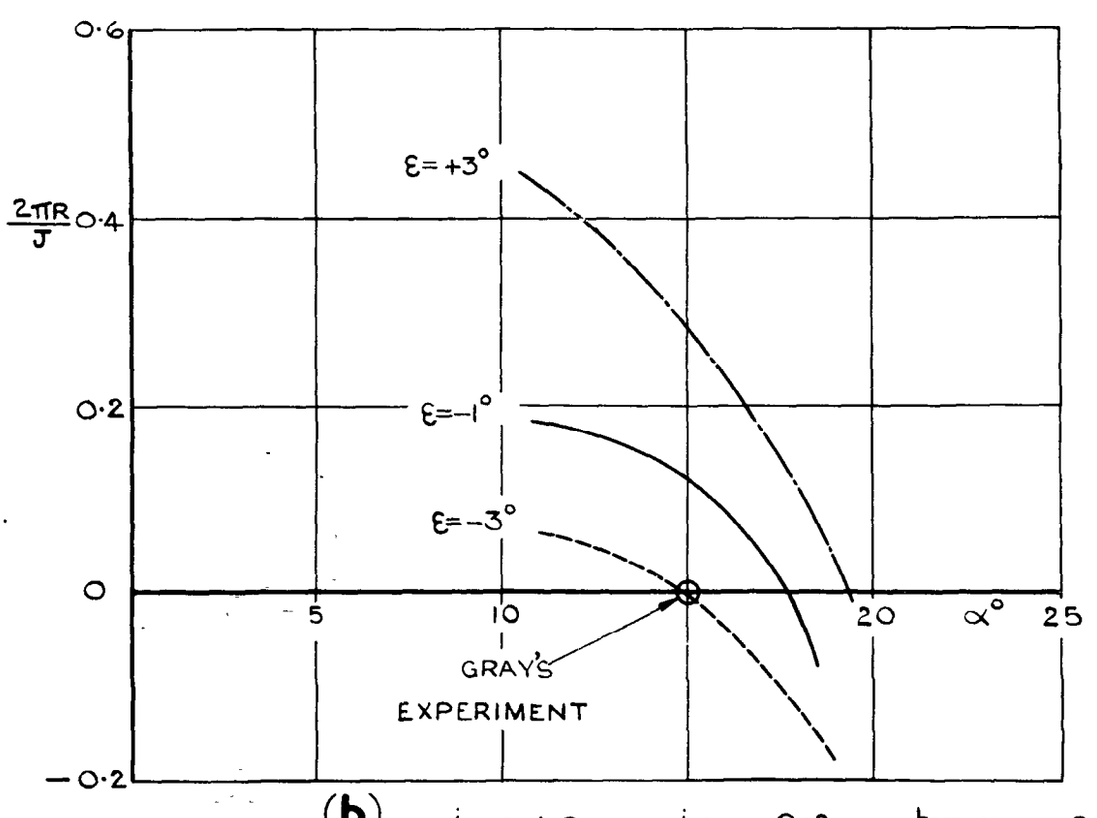

(b.) $i_{c_0} = 1{\cdot}0$, $i_{A_0} = 0{\cdot}2$, $\tan.\gamma_e = -0{\cdot}25$

C.G. AT $0{\cdot}535\, c_0$

FIG. 3. VARIATION OF LOG DEC. WITH INCIDENCE FOR GRAY'S SIMPLE MODELS

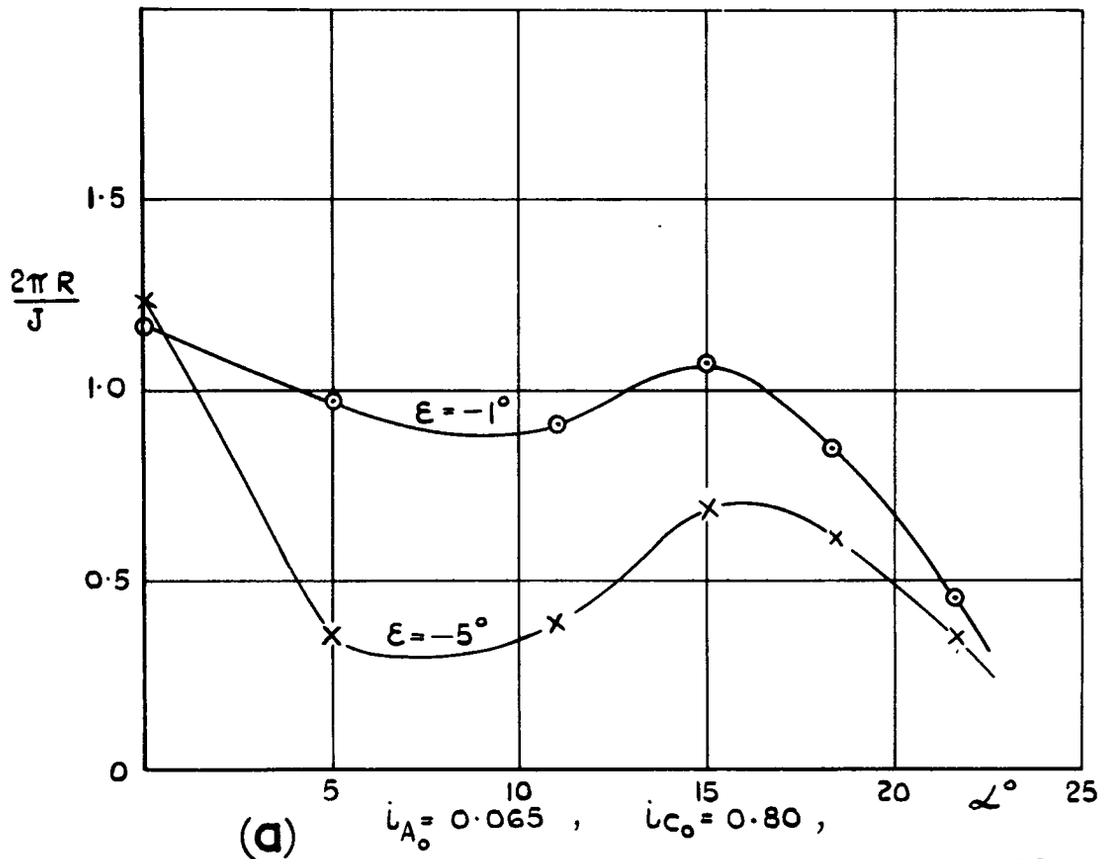

(a) $i_{A_0} = 0.065$, $i_{C_0} = 0.80$,

THEORETICAL RESULTS FOR ε = −1° AND −5°

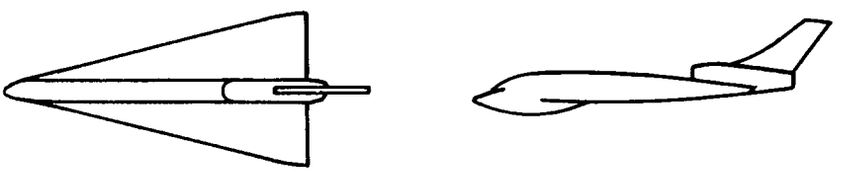

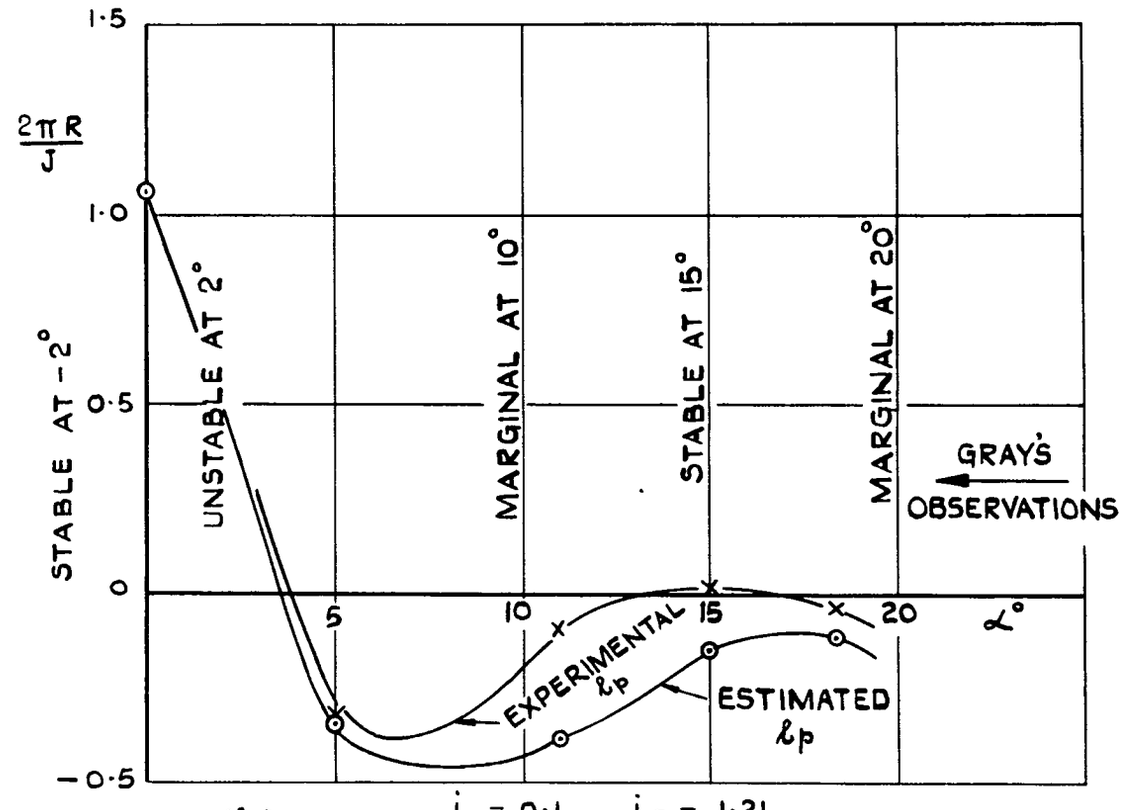

(b) $i_{A_0} = 0.1$ $i_{C_0} = 1.21$

THEORETICAL AND EXPERIMENTAL RESULTS FOR ε = − 8°

FIG.4. EFFECT OF INCLINATION OF INERTIA AXIS

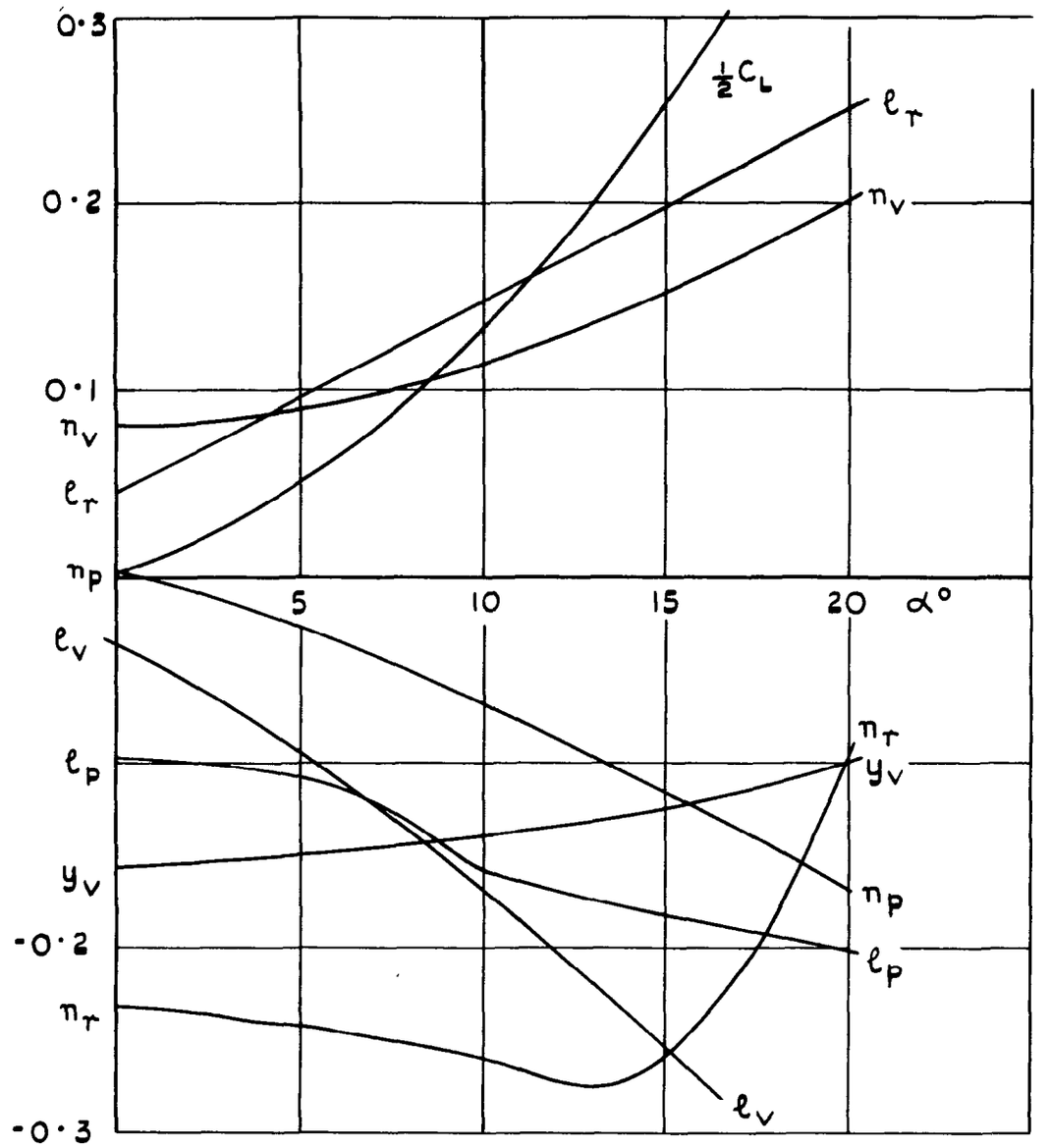

FIG. 5. DERIVATIVES FOR OGEE WING DESIGN (WING 15 OF REF 8, WITH TRIANGULAR FIN.)

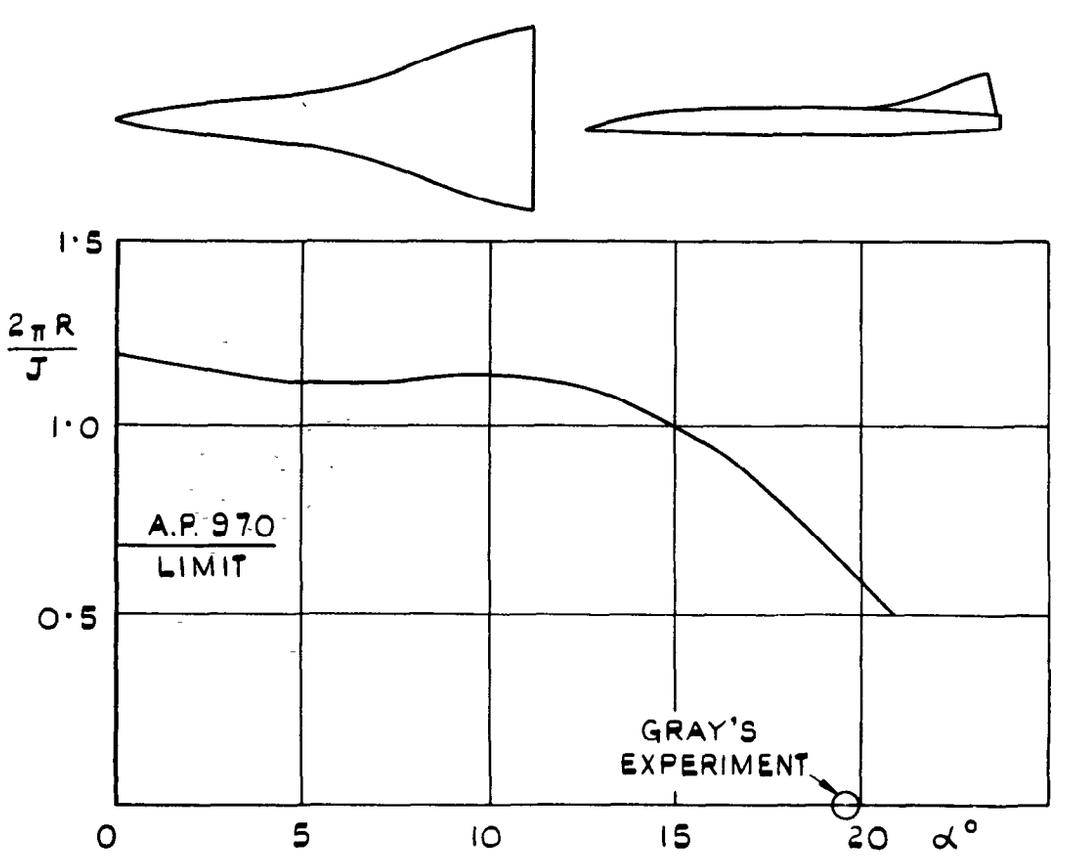

FIG. 6. LOG DEC OF OGEE WING DESIGN.

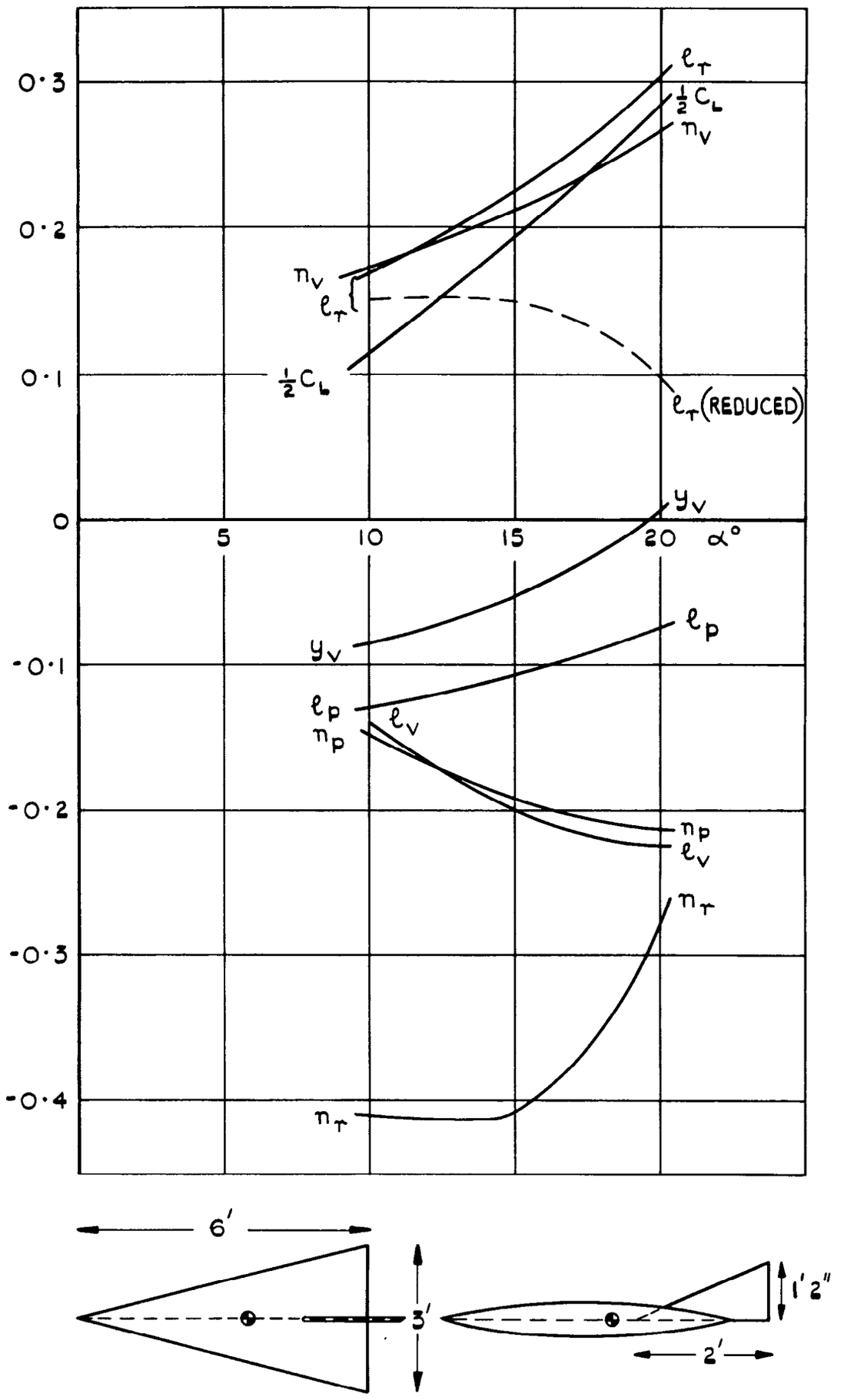

FIG. 7. DERIVATIVES FOR BISGOOD'S MODELS (REF. 7)

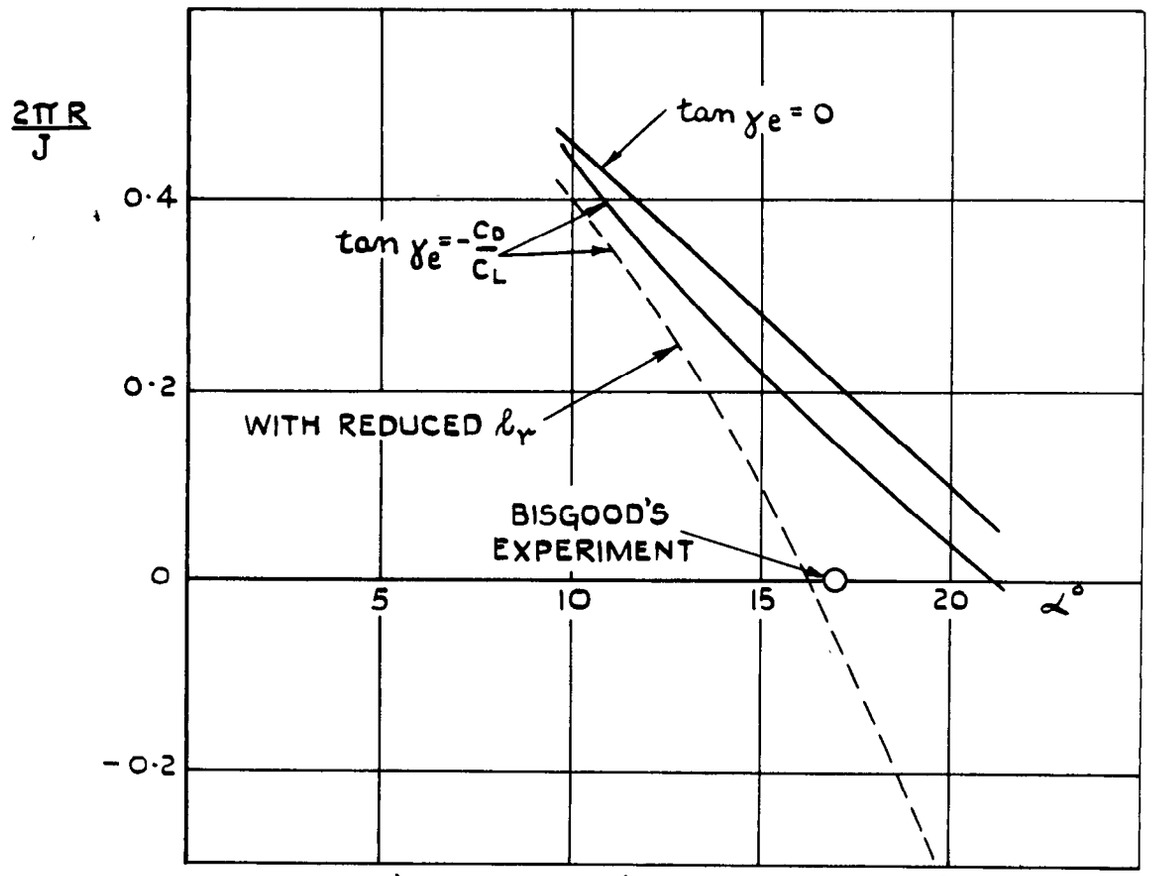

(a) $i_{A_0} = 0.11$, $i_{C_0} = 0.82$, $\varepsilon = -1°$
(INERTIA RATIO 7 IN REF. 7.)

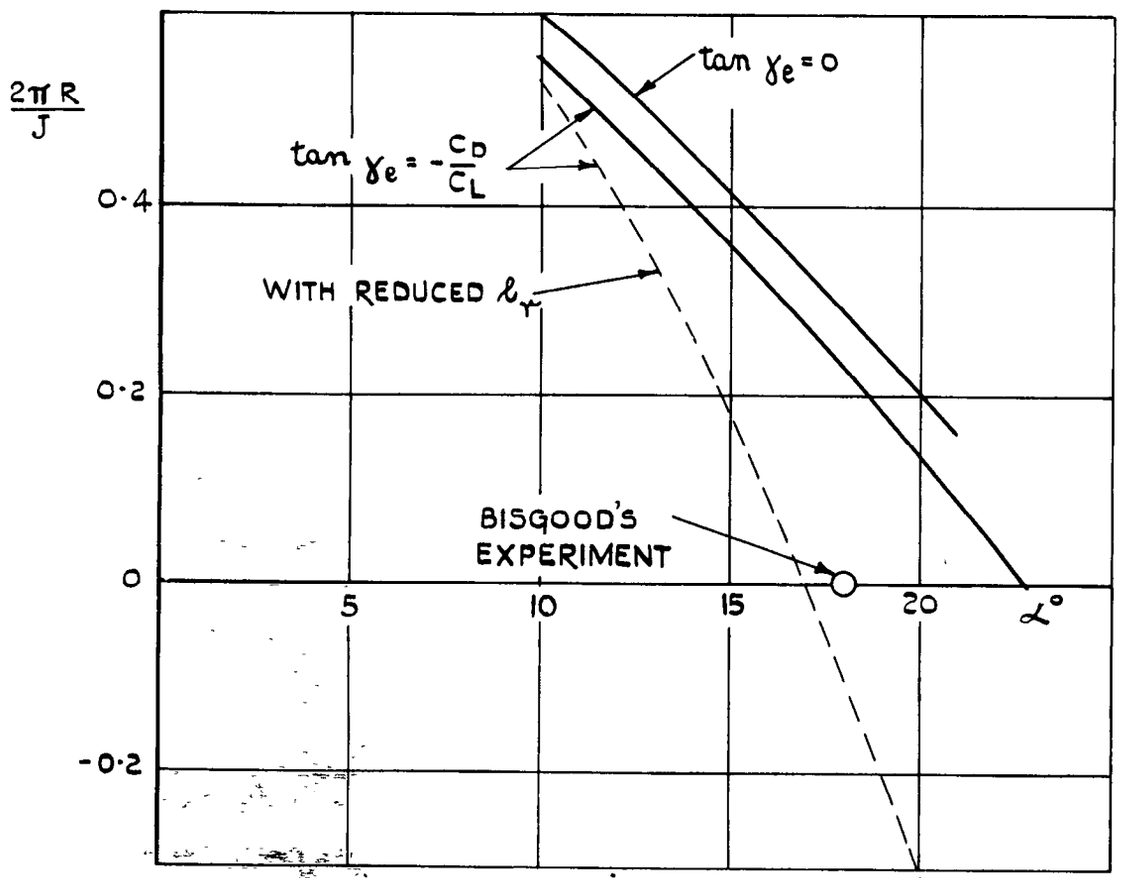

(b) $i_{A_0} = 0.10$, $i_{C_0} = 1.41$ $\varepsilon = -1°$
(INERTIA RATIO 13 IN REF. 7)

FIG.8. VARIATION OF LOG DEC. WITH INCIDENCE FOR BISGOOD'S FREE FLIGHT MODELS

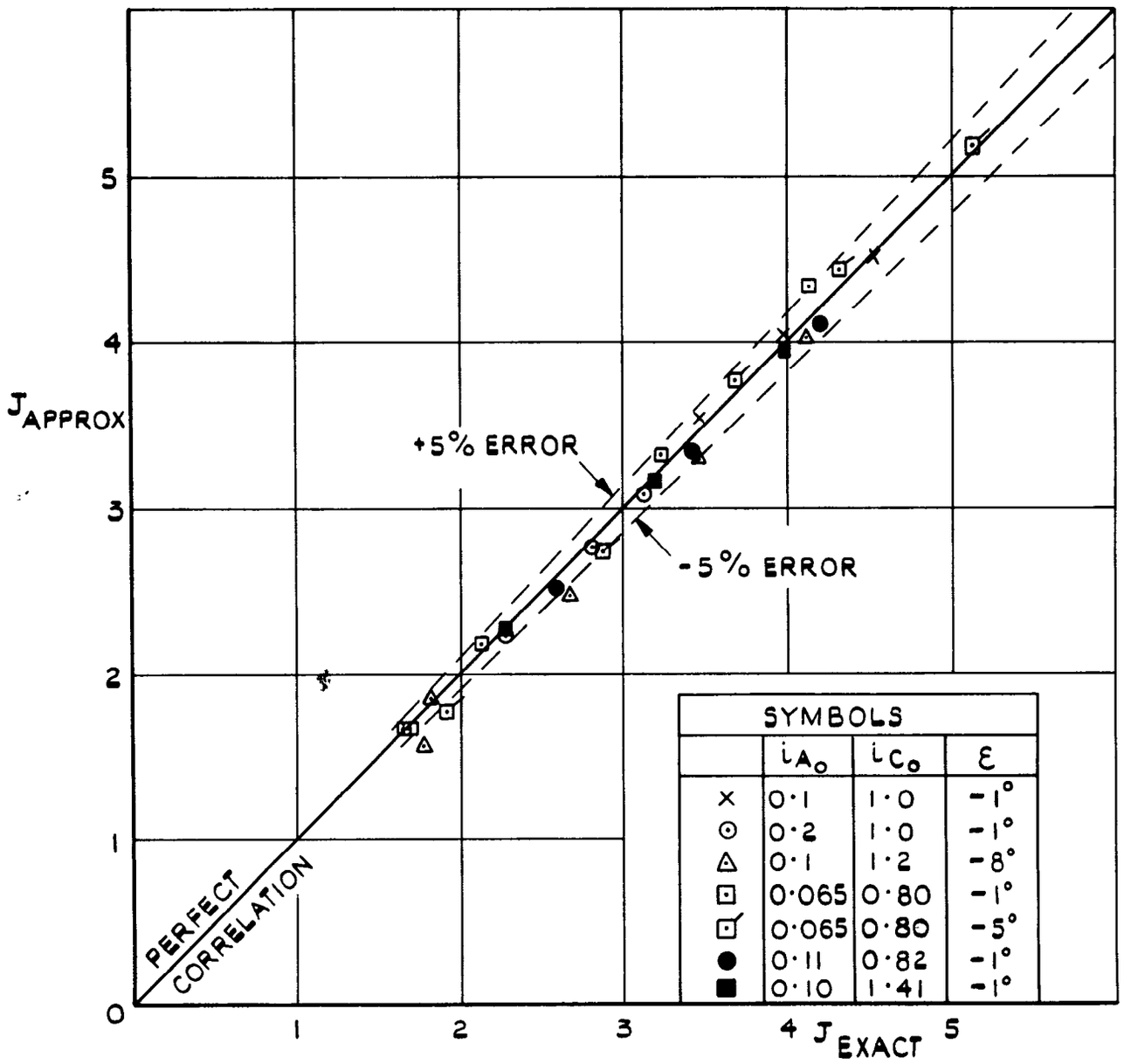

FIG. 9. CORRELATION OF EXACT AND APPROXIMATE VALUES OF FREQUENCY (EQUATION 2)

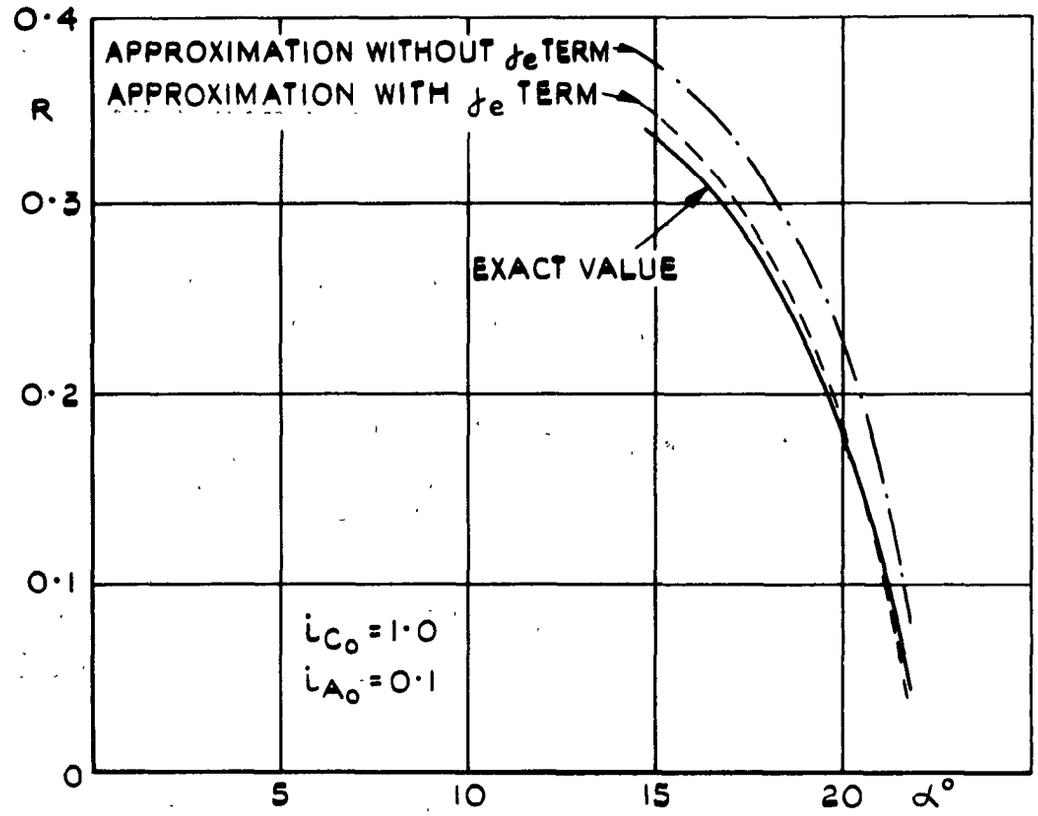

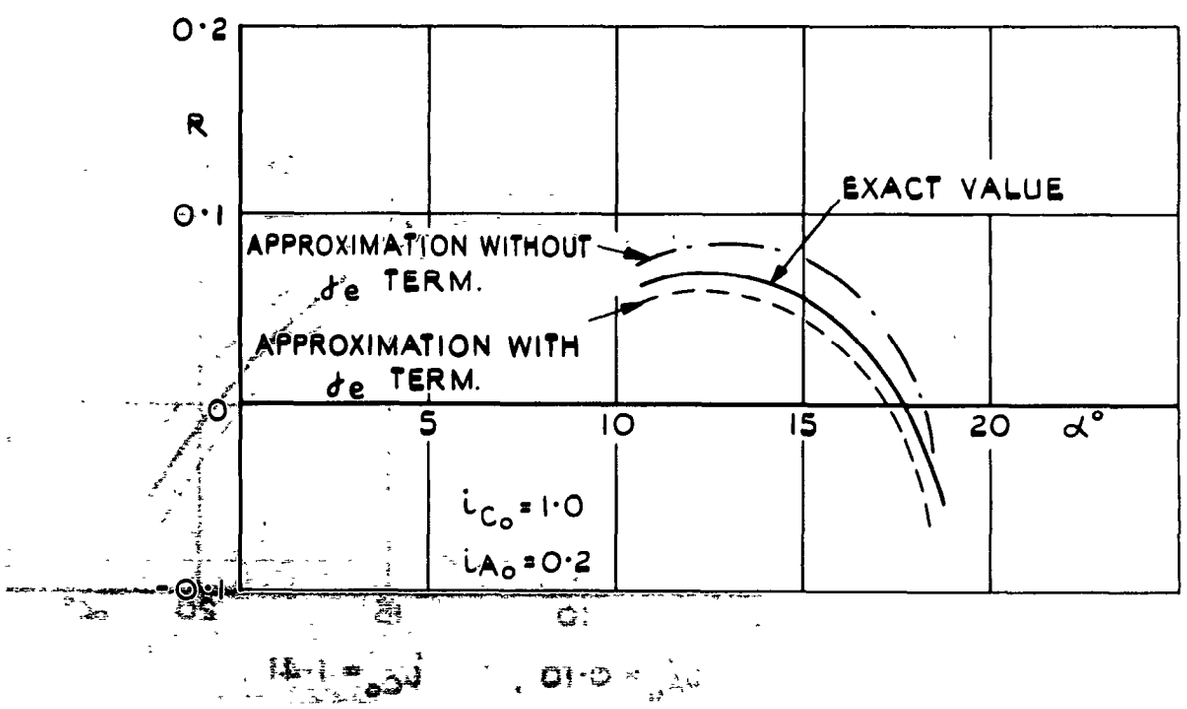

FIG. 10(a) COMPARISON OF EXACT VALUE OF DAMPING WITH APPROXIMATION (EQUATION 3) (GRAY'S CONFIGURATIONS.)

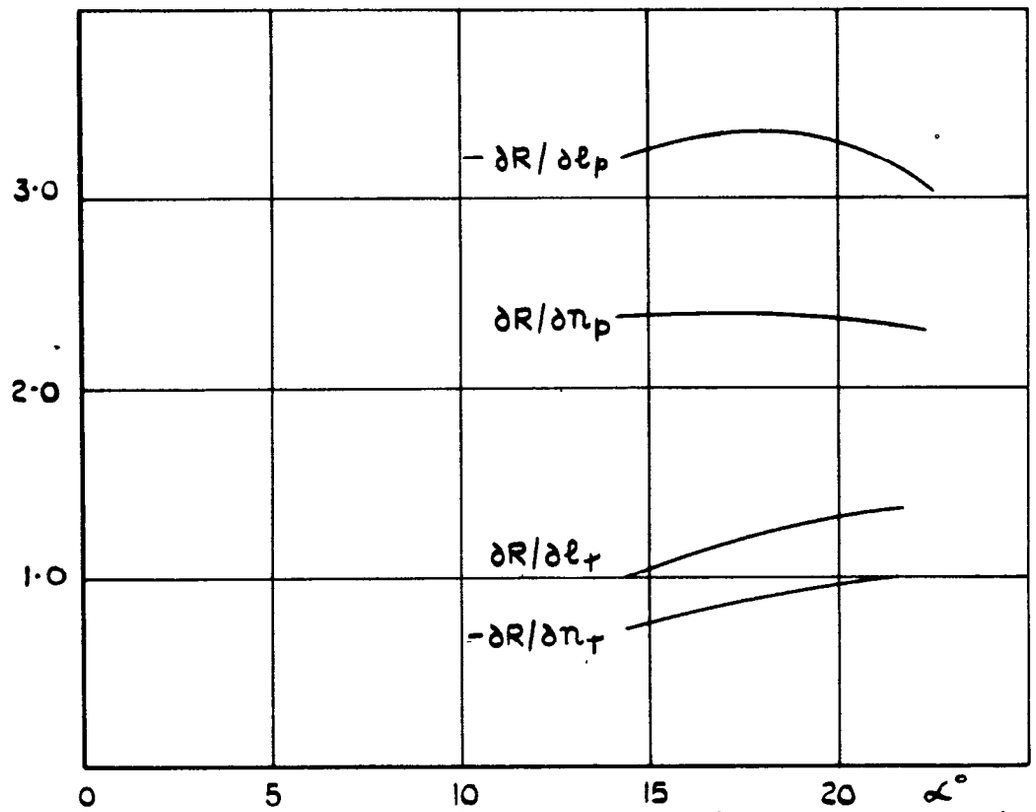

(a) $i_{A_0} = 0.1$, $i_{C_0} = 1.0$, (GRAY'S CONFIGURATION)

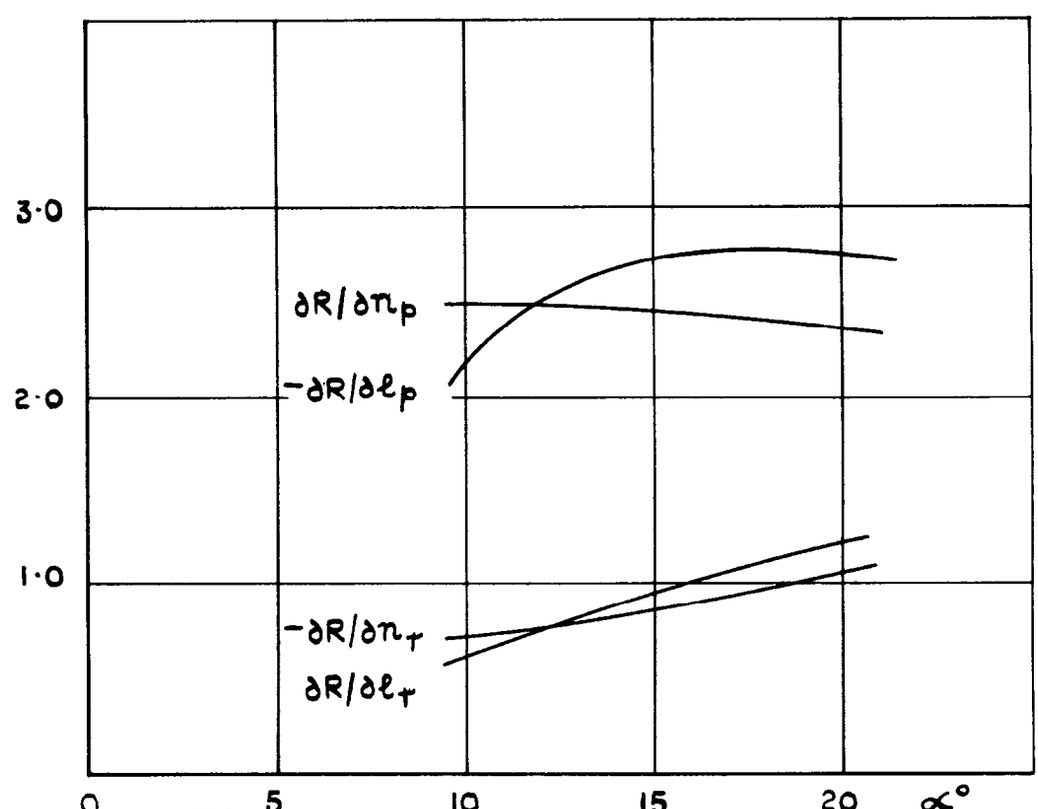

(b) $i_{A_0} = 0.11$, $i_{C_0} = 0.82$, (BISGOOD'S CONFIGURATION)

FIG.12. APPROXIMATE VALUES OF VARIATION OF DAMPING WITH ROTARY DERIVATIVES

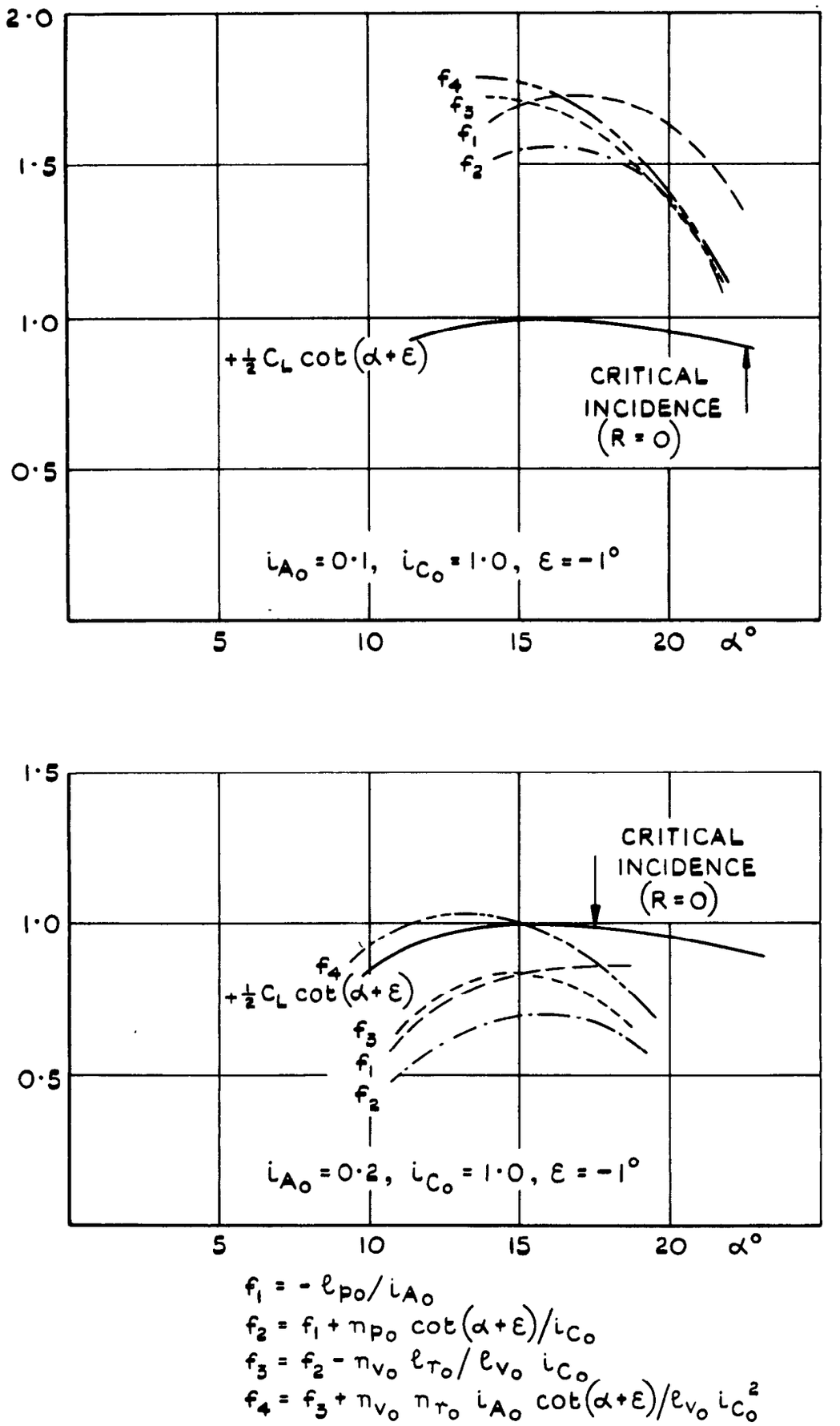

FIG. 13. COMPARISON OF CRITERIA FOR DETERMINATION OF CRITICAL ANGLE OF INCIDENCE $\frac{1}{2}C_L \cot(\alpha+\varepsilon) = f_1$ TO f_4 (GRAY'S CONFIGURATIONS)

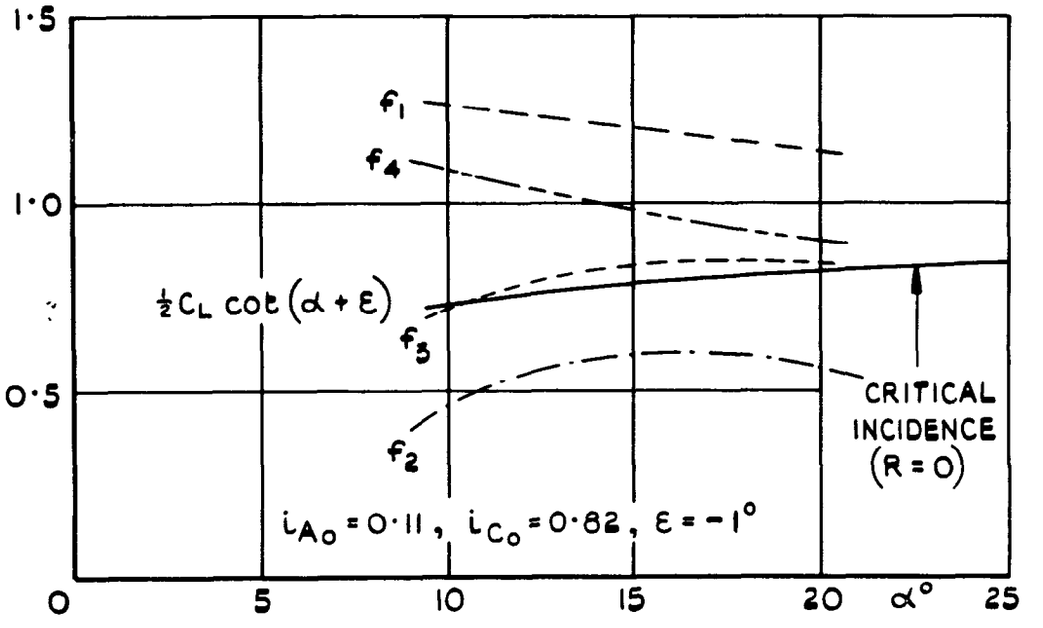

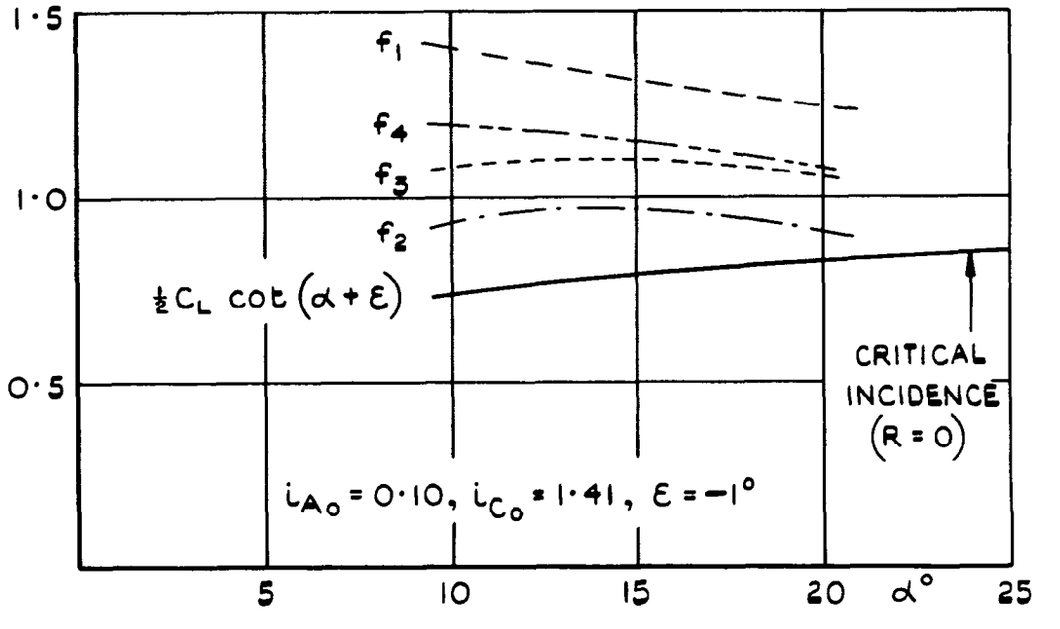

$$f_1 = -\ell_{p_0}/i_{A_0}$$
$$f_2 = f_1 + n_{p_0}\cot(\alpha+\varepsilon)/i_{C_0}$$
$$f_3 = f_2 - n_{V_0}\,\ell_{T_0}/\ell_{V_0}\,i_{C_0}$$
$$f_4 = f_3 + n_{V_0}\,n_{T_0}\,i_{A_0}\cot(\alpha+\varepsilon)/\ell_{V_0}\,i_{C_0}^2$$

FIG. 13. COMPARISON OF CRITERIA FOR DETERMINATION OF CRITICAL ANGLE OF INCIDENCE $\frac{1}{2}C_L\cot(\alpha+\varepsilon) = f_1$ TO f_4 (BISGOOD'S CONFIGURATIONS)

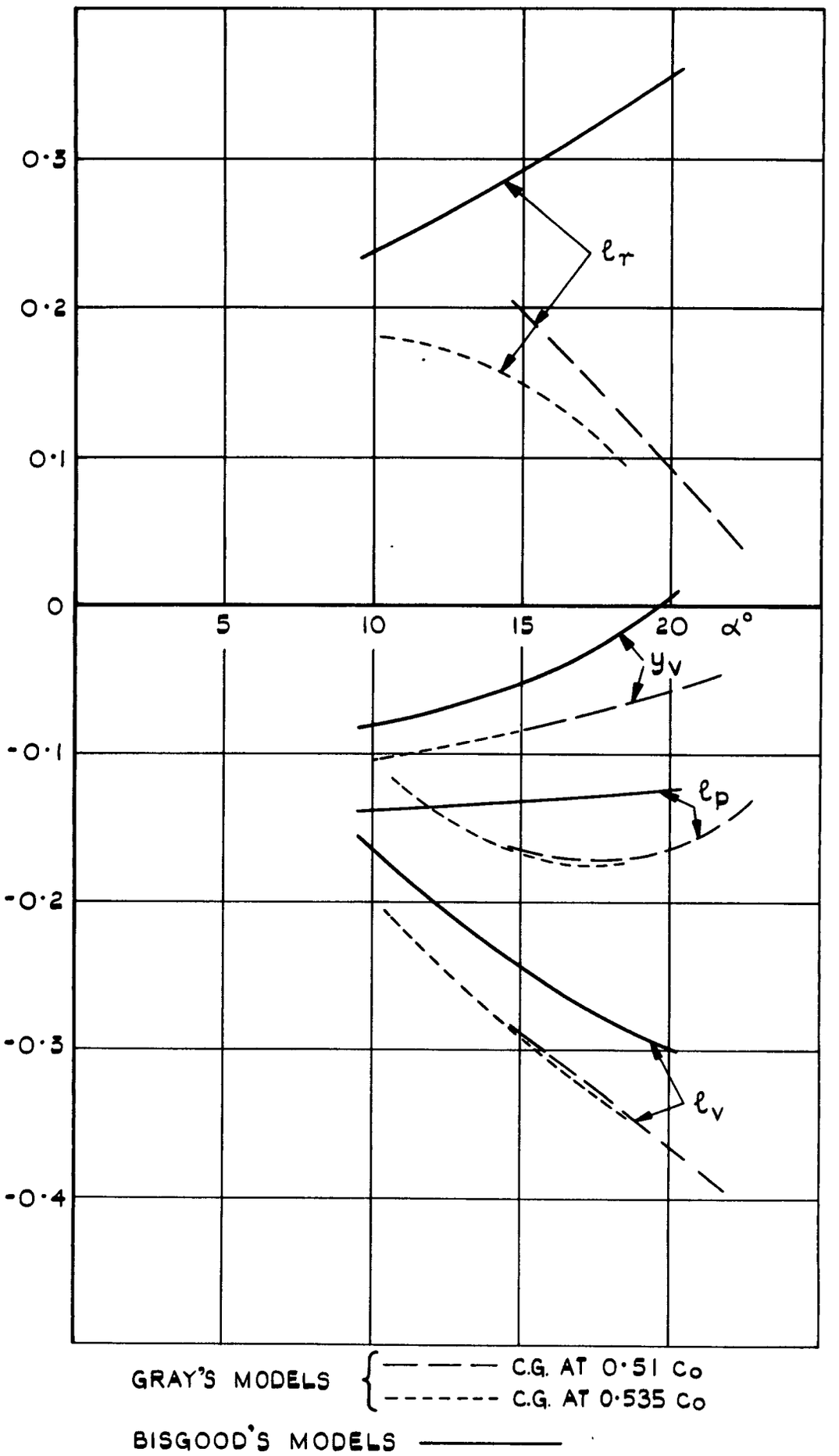

(a) ROLLING MOMENTS AND SIDE FORCE.

FIG. 14. DERIVATIVES REFERRED TO PRINCIPAL INERTIA AXES ($\varepsilon = -1^\circ$)

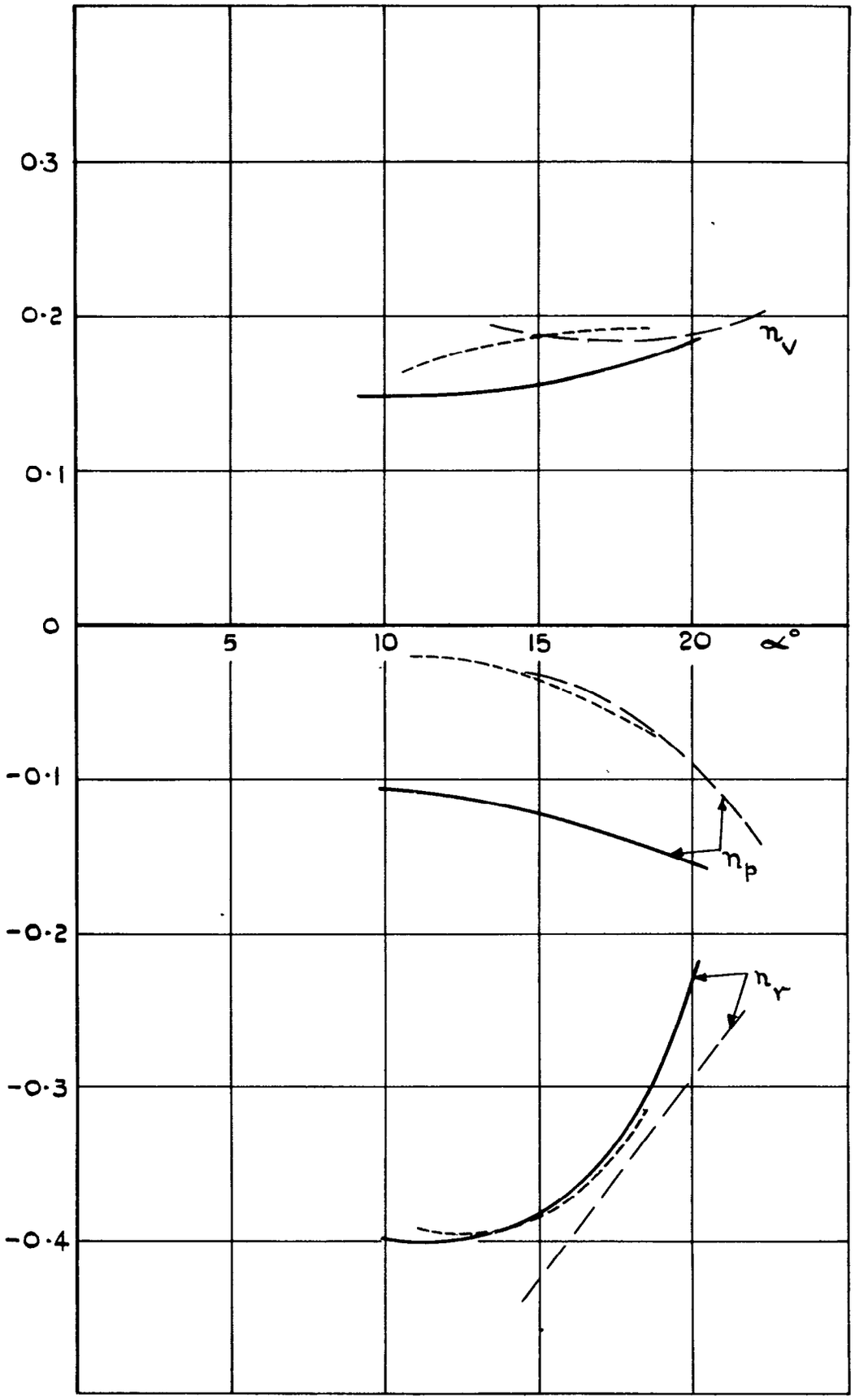

GRAY'S MODELS { — — — — C.G. AT 0·51c_0
---------- C.G. AT 0·535c_0.

BISGOOD'S MODELS ————

(b) YAWING MOMENTS

FIG.14. DERIVATIVES REFERRED TO PRINCIPAL INERTIA AXES ($\varepsilon = -1^\circ$)

Printed in England for Her Majesty's Stationery Office by the Royal Aircraft Establishment, Farnborough. Dd.125875. K.4.

ARC C.P. No.845

533.693.3:
533.6.013.413:
533.6.013.42:

THE LATERAL OSCILLATION OF SLENDER AIRCRAFT.
Ross, A.J. June 1962.

Theoretical estimates of the angle of incidence at which the damping of the Dutch-roll oscillation of various slender-wing configurations becomes zero are derived and shown to agree well with the critical angle of incidence, observed experimentally, at which free-flying models undergo a sustained oscillation.

Some approximations to the frequency and damping of the oscillation are compared with the exact values, with satisfactory agreement. A criterion for critical angle of incidence is obtained, the complexity of which depends mainly on the inertia distribution of the aircraft.

UNCLASSIFIED

ARC C.P. No.845

533.693.3
533.6.013.413:
533.6.013.42:

THE LATERAL OSCILLATION OF SLENDER AIRCRAFT.
Ross, A.J. June 1962.

Theoretical estimates of the angle of incidence at which the damping of the Dutch-roll oscillation of various slender-wing configurations becomes zero are derived and shown to agree well with the critical angle of incidence, observed experimentally, at which free-flying models undergo a sustained oscillation.

Some approximations to the frequency and damping of the oscillation are compared with the exact values, with satisfactory agreement. A criterion for critical angle of incidence is obtained, the complexity of which depends mainly on the inertia distribution of the aircraft.

UNCLASSIFIED

UNCLASSIFIED

ARC C.P. No.845

533.693.3:
533.6.013.413:
533.6.013.42:

THE LATERAL OSCILLATION OF SLENDER AIRCRAFT.
Ross, A.J. June 1962.

Theoretical estimates of the angle of incidence at which the damping of the Dutch-roll oscillation of various slender-wing configurations becomes zero are derived and shown to agree well with the critical angle of incidence, observed experimentally, at which free-flying models undergo a

Some approximations to the frequency and damping of the oscillation are compared with the exact values, with satisfactory agreement. A criterion for critical angle of incidence is obtained, the complexity of which depends mainly on the inertia distribution of the aircraft.

Published by
HER MAJESTY'S STATIONERY OFFICE

To be purchased from
49 High Holborn, London W.C.1
423 Oxford Street, London W.1
13A Castle Street, Edinburgh 2
109 St. Mary Street, Cardiff
Brazennose Street, Manchester 2
50 Fairfax Street, Bristol 1
35 Smallbrook, Ringway, Birmingham 5
80 Chichester Street, Belfast 1
or through any bookseller

C.P. No. 845

S.O. CODE No. 23-9016-45